Effect of SiO_2 nano particle dispersion on the structural and dielectric behaviour of lyotropic liquid crystalline phase

A

Thesis

Submitted in the partial fulfilment of requirement for the degree of

MASTER OF TECHNOLOGY

In

MATERIALS AND METALLURGICAL ENGINEERING

By

Vijay Kumar Baliyan

(600902013)

UNDER THE SUPERVISION OF

Dr. K. K. Raina

School of Physics and Materials Sciences

Thapar University, Patiala, (Punjab)

June-2011

CERTIFICATE

This is certify that the thesis entitled ***"Effect of SiO_2 nano particle dispersion on the structural and dielectric behaviour of lyotropic liquid crystalline phase"*** submitted by **Vijay Kumar Baliyan** in the partial fulfilment of the requirement for the award of degree of **M.Tech** in **Material Science and Metallurgical Engineering** from the School of Physics and Material Science, Thapar University, Patiala is a record of candidate's own work carried out by him under my supervision and guidance. The experimental matter embodied in this report has not been submitted in part or full to any other university or institute for the award of any degree.

Supervisor

Dr. K.K. Raina
Deputy Director,
Distinguished Professor,
Thapar University, Patiala

Countersigned by

Dr. O.P. Pandey
Professor & Head
Thapar University
Patiala, Punjab

Dr. S.K. Mohapatra
Dean of Academic Affairs
Thapar University,
Patiala, Punjab

ACKNOWLEDGEMENT

My heartfelt thanks are due to my advisor, ***Dr. K. K. Raina****,* ***Distinguished Professor and Deputy Director, Thapar University, Patiala*** *who believes in me and who has guided me to scale heights during my work. Their unique inimitable style has left an indelible impression on me. Their constant encouragement helps and reviews during the course of investigation are invaluable. Nevertheless it helps me acquire and develop some of the skills and intricacies of good independent research. I thank him for his great patience, constructive criticism and myriad useful suggestions apart from invaluable guidance to me.*

My greatest thanks are to ***Dr.O.P. Pandey, Prof. & Head, School of Physics and Material Science, Thapar University, Patiala*** *for his encouragement and execution of thesis work.*

I am highly greatful to ***Dr. Kulvir Singh, Asst. Prof., School Of Physics And Material Science, Thapar University, Patiala*** *for their kind help and valuable suggestions and special attention throughout my work.*

I am also indebted to ***Dr. Manoj Sharma, Associate Professor and PG incharge, School of Physics and Materials Science*** *for their full motivation and appreciation to my work.*
I am also thankful to all the faculty members of School of Physics and Materials Science, for their constructive suggestions at different stages of my work.

It gives me immense pleasure to express my special thanks to ***Mr. Ravi Shukla (Ph.D. Scholar)****, who always took keen interest in guiding me during my work. I wish to express my warm and sincere thanks to Research Scholars* ***Miss Neeraj Sharma****,* ***Rishi Kumar****,* ***Miss Supreet, Miss Ramneek, Miss Gurpreet*** *and my colleagues* ***Richa sharma, Geetanjali, Vipin Sharma and Arvind Kumar*** *for their support and their timely help and valuable discussions.*

I owe my sincere thanks to all the staff members of School of Physics and Materials Science for their support and encouragement. Last but not the least; I would like to thank all my ***family members and friends*** *for their moral support that kept my spirit up during the endeavour.*

VIJAY KUMAR BALIYAN

ABSTRACT

Present study is an effort to understand the effect of SiO_2 nano- particles (5-15 nm) on the variety of lyotropic liquid crystalline (LLC) phases obtain from cationic and anionic [Cetyl perydinium chloride ($C_{21}H_{38}NCl$), N-Cetyl-NNN, Trimethyl ammonium bromide ($C_{19}H_{42}BrN$) and Sodium dodecyl Sulphate [($C_{12}H_{25}SO_4Na$)] amphiphilic molecules in the non-aqueous medium of the protic polar solvent ethylene glycol (EG). The prepared pure and dispersed LLC phases were characterized by using polarizing optical microscope (POM), X-ray diffractometer (XRD), LCR meter and Fourier transform infra-red spectroscopy (FTIR) to examine the optical, structural, dielectric and chemical behvaiour. Morphological and structural characterizations reveal that addition of Si particles does not affect the ordering and structure of the LLC phases in any case. Lamellar to hexagonal phase transition has been noticed in the CTAB based sample dispersed with 0.5wt% Si. It was found that dielectric permittivity found to be decreased with addition of Si particles in LLC phases derived from cationic surfactants, however, addition of Si particles in SDS based samples enhance the permittivity. No chemical interaction has been noticed in the Si dispersed samples.

CONTENTS

LIST OF FIGURES

Chapter 1

Chapter 2

Chapter 3

Figure 4.2(a) X-ray diffraction patterns of CPCL:EG:Si systems

Figure 4.2(b) X-ray diffraction patterns of CTAB:EG:Si systems

Figure 4.2(c) X-ray diffraction pattern of SDS:EG: Si systems

Figure 4.3(a) Variation of relative permittivity with frequency for CPCL:EG:Si systems room temp.

Figure 4.3(b) Variation of tanδ with frequency for CPCL:EG:Si systems room temp.

Figure 4.3(c): Variation of relative permittivity with temperature for CPCL:EG:Si systems at 100 Hz.

Figure 4.3(d): Variation of tanδ with frequency for CPCL:EG:Si systems at100 Hz.

Figure 4.3(e) Variation of relative permittivity with frequency for CTAB:EG:Si systems room temp

Figure 4.3(f) Variation of tanδ with frequency for CTAB:EG:Si systems room temp.

Figure 4.3(h): Variation of tanδ with frequency for CTAB:EG:Si systems at100 Hz.

Figure 4.3(i): Variation of relative permittivity with frequency for SDS:EG:Si systems room temp

Figure 4.3(j) Variation of tanδ with frequency for SDS:EG:Si systems room temp.

Figure 4.3(k): Variation of relative permittivity with temperature for SDS:EG:Si systems at 100 Hz.

Figure 4.3(i): Variation of tanδ with frequency for SDS:EG:Si systems at100 Hz.

Figure 4.3(m): Variation of relative permittivity of all pure samples with respect to frequency at room temperature

Figure 4.3(n): Variation of tanδ Vs frequency for all pure samples at room temperature.

Figure 4.3(o): Variation of relative permittivity of all systems at Si 0.05% with respect to frequency at room temperature

Figure 4.3(p): Variation of tanδ Vs frequency at room temperature for all systems dispersed with Si 0.05wt%.

Figure 4.3(q): Variation of relative permittivity of all systems at Si 0.1% with respect to frequency at room temperature.

Figure 4.3 (r): Variation of tanδ Vs frequency at room temperature for all systems dispersed with Si 0.1wt%.

Figure 4.3(s) Variation of relative permittivity of all samples at Si 0.5% with respect to frequency at room temperature.

Figure 4.3 (t): Variation of tanδ Vs frequency at room temperature for all systems dispersed with Si 0.5wt%.

Figure 4.4(a): FTIR spectra of CPCL:EG pure and Si particle dispersed systems

Figure 4.4(b): FTIR spectra of CTAB:EG pure and Si particle dispersed systems

Figure 4.4(c): FTIR spectra of SDS:EG pure and si particle dispersed systems

CHAPTER 1

INTRODUCTION

1.1 Review

Liquid crystals are intermediate state of matter or mesophases, halfway between an isotropic liquid and a solid crystal [1]. In nature, some substances or even mixture of substances, exhibits these mesomorphic states. This picture leads to the concept of ordering in a solid crystal. The basic units display translation long-range order with the centre of mass of atoms or molecules located on a crystal lattice; in some cases, the basic units also display orientational order. In an isotropic liquid, the basic unit do not present either positional or orientational long-range order. From an ordering limit (solid state) to the other (isotropic liquid), there may exist many different situations. In liquid crystals, the basic units display orientational order and even positional order along some directions. These materials flow like an isotropic fluid and have characteristic optical properties of solid crystals. Liquid crystals are of two types

1. Thermotropic liquid crystals
2. Lyotropic liquid crystals

In thermotropic liquid crystals the basic units are molecules, and phase transitition depends on temperature and pressure. Pronounced shape anisotropy is the main feature of molecules which gives rise to a thermotropic mesophases. Rods, disks, and banana-shaped are examples of molecular geometries associated with the thermotropic liquid crystals. Besides pure substances, mixtures of molecules can also present thermotropic properties. Thermotropics are widely used in displays of low energy cost and in many sensor devices.

Lyotropic liquid crystals are mixture of amphiphilic molecules and solvents at given temperature and relative concentrations. The mesomorphic properties change with temperature, pressure and the relative concentration of the different component of the mixture. An important feature of lyotropics, turning them different from thermotropics is the self assembly of the amphiphlic molecules as super molecular structures, which are the basic

unit of these mesophases. Although there are not many devices based on lyotropics, there physical-chemical properties have an interesting interface with biology and the understanding of these properties has been relevant for improving some technological aspects of cosmetics, soap, food, crude oil recovery, and detergent production.

It is interesting to point out that there is a family of complex isotropic fluids, which have been called micro-emulsions, whose characteristics, in some respects, overlap with those of lyotropics. Micro-emulsions are mixture of oil, water and amphiphile molecules which beheave as an optically isotropic and thermodynamically stable liquid solution [2-4]. These systems differ from the emulsions which are kinetically stable. In micro emulsion, the typical size of basic unit (self assembled molecular aggregates) is about 10 nm, which makes the mixture transparent to visible light. On the other hand, emulsion diffuse visible light, displaying a milky or cloudy aspect, which indicates that their basic unit are larger, typically a micro meter dimensions. The conceptual boundaries between lyotropics, in particular the isotropic phases and micro-emulsions are not sharp. Sometimes, the isotropic phases of same mixture, with oil as one of the component, are included in different side of this border. In order to differentiate them, we point out that micro-emulsions are two phase systems and lyotropic are one phase systems.

1.2 Hydrophobic and hydrophilic effects

Water is present in almost all the lyotropic mixtures. The behavior of a molecule of a given substance with respect to the water molecules plays a crucial role in the formation of a lyomesophase.

In the field of complex and superamolecular fluids, the concepts of hydrophobic (hates water) and hydrophilic (loves water) refer to the affinity of a particular molecule with respect to the water molecules. Sometimes these effects are treated as interactions, but this is not the case. The involved interactions are of electrostatic nature, since water molecules have a permanent dipole moment [5]. From the point of view of electrostatic dipole dipole interactions, similar molecules or even part of molecules, tends to be together. Therefore polar molecules are easily dissolved in water and non polar substances (paraffin) are difficult to be dissolved in water.

The mechanism of ordering the water molecules based on hydrogen bonds, play an essential role in these effects [6]. At room temperatures (~25^{o}C), the water molecules arrange themselves as an isotropic liquid. A distortion of this structural arrangement which cost

energy, take place upon the introduction of the solute. If the solute is polar, some energy compensation occurs and the dilution becomes possible. On the other hand, if the solute is non-polar, no energy compensation occurs and the dilution is difficult.

1.3 Amphiphilic molecules

Amphiphilic molecules are always present in the composition of lyotropic liquid crystals. They may be synthesized for different purposes ranging from interests in basic science to technological applications in various branches of industry.

The name amphiphilic comes from the Greek prefix amphi, which means both or double, and the word phile, which means like or love. This word is applied to a compound that displays a double "preference," "loving both," from the electrostatic point of view. It is used to name a molecule with a polar water soluble group attached to a water–insoluble hydrocarbon chain. An example of this type of molecule, sodium decylsulfate (NadS or SdS), is illustrated in Fig. 1.1

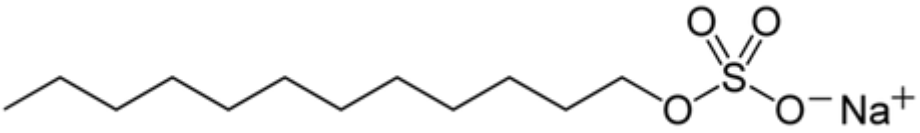

Figure: 1.1 Amphiphilic molecule of sodium decylsulphate (NadS)

These molecules are surfactants (from surface active agent) since they can modify the properties of surfaces and interfaces between the different mediea, as solid-liquid or liquid-gas interfaces. There are different types of natural and chemically synthesized amphiphilic molecules; anonic amphiphiles (soap of fatty acids; e.g., potassium laurate), detergent (e.g. sodium decylsulphate); cationic amphiphiles (e.g. hexadecyltrimethylammonium bromide); nonionic amphiphiles (e.g. pentaethyleneglycoldodecyl ether); and zwitterionic amphiphiles (which develops an electric dipole in the presence of water; e.g. lysolectihin). In fig.1.2, we sketch some examples. Another type of surfactant molecules that give rise to a lyotropic mesophases are the anelydes. These molecules are able to selectively complex some metallic ions [7], which are then incorporated in their structure.

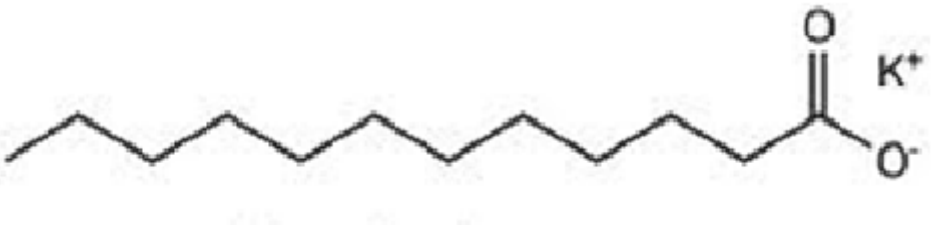

(a) Potassium laurite

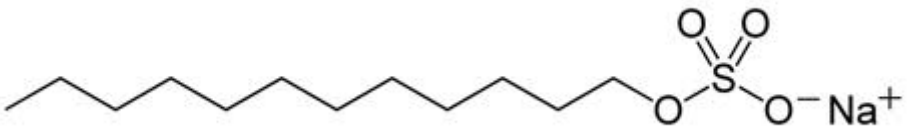

(b) SLS (sodium laurylsulphate)

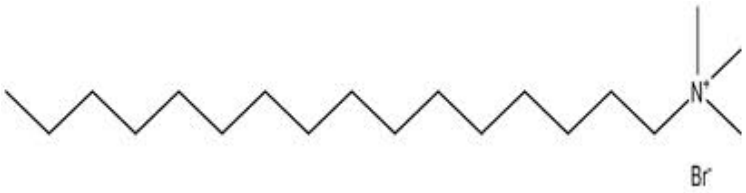

(c) HTAB

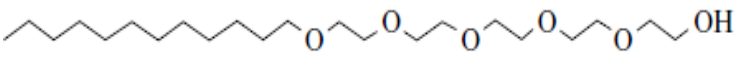

(d) Nonionic fatty alchol ethoxylate

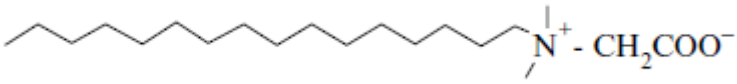

(e) Zwitterionic Betaine

Fgure: 1.2 Various amphiphilic molecules

It is important to note that a polar group is not always required to be hydrophilic (nor in a non-polar group always hydrophobic). The topology of the molecule and its insertion into the water network is also important to characterize the solubility of water [8].

1.4 Lyotropic mixture

Under suitable conditions of temperature and relative concentrations, mixtures of amphiphilic molecules and solvents can give rise to a lyotropic mesophases. In this type of system, amphiphilic molecules form self assembled superstructures of several shape anisotropies and sizes. Let us first classify lyotropics into three big families:

(a) Micellar systems, with molecular aggregates, called micelles, of small shape anisotropy, in fig. 1.3 (a). These micelles are aggregates of amphiphilic molecules, with typical dimensions of about 10 nm shape anisotropy of order 1:2 in linear dimensions.

(b) System with aggregates of large shape anisotropy, of typical order 1:100 in terms of linear dimensions. These aggregates are sometimes called infinite, but we do not use this nomenclature.

(c) Bicontinuous system, in which the amphiphilic molecules self assemble as a three dimensional continuous structure at large scale (10^{-3} nm). Fig.1.4 shows a sketch of a bicontinuous molecular aggregate with cubic symmetry.

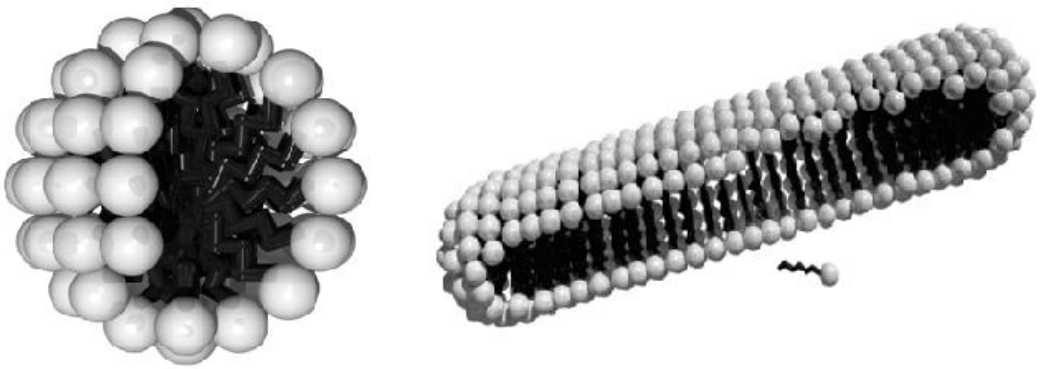

(a) (b)

Figure: 1.3 (a) Micelles of small shape and (b) Cyclindrical micelles

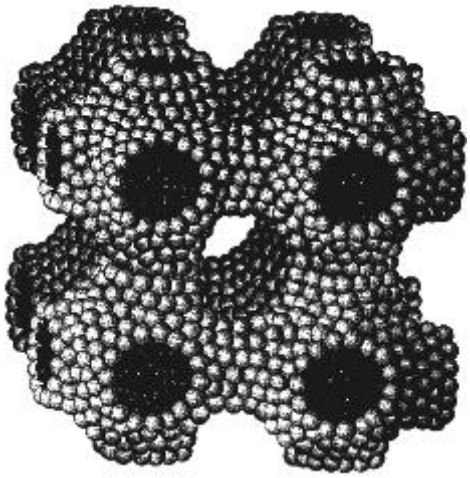

Figure: 1.4 Sketch of a bicontinuous molecular aggregate with a cubic symmetry

1.5 Self assembled system

In the case of amphiphilic molecules and a solvent, one interesting concept is the *critical micellar concentration*, CMC, [9]. It is defined as the concentration of amphiphilic molecules above which they self-assemble into micelles. Let C be the concentration of amphiphilic molecules in the solution of amphiphiles and a solvent. For C is less than CMC, the amphiphilic molecules remain isolated without the formation micelles. For C is greater than CMC, the fraction of isolated amphiphilic molecules remains almost constant and the concentration of micelles increase with C. The hydrophobic/hydrophilic effects are the most important mechanism of micelles formation. In water based mixtures, the formation of micelles can also be understood in terms of the entropy of the structured water, since for concentration larger than CMC, the aggeration of the amphiphilic molecules increases the water entropy [10].

1.6 Surfactant start to form micelles

Temperature as an important parameter, conditions the appearance of certain phases, both in thermotropic and lyotropic liquid crystals, but because lyotropics are solutions of at least two compounds, temperature is not the determinant parameter, but the concentration. Further discussions about lyotropics imply water as high polarity solvent [18] and whenever solutions will contain more than two compounds, it will be specified.

Up to a certain concentration i.e. CMC, lyotropics did not yet aggregate since the molecular disorder still existing. At the CMC value, a spontaneous organization network of the amphiphilic molecules begins and molecular aggregates of colloidal sizes appear; they have been called "association micelles". But the solution did not yet show liquid crystals behavior and is called "isotropic micellar solution" (IS). If the concentration increases more, lyotropic specific structures appear with a structural order even up to three dimensions and the solution becomes an anisotropic one, more or less viscous. Only in this case, the micellar solution is a liquid crystal. The micellar aggregates contain a large number of monomers depending on the chemical composition of the surfactant, the aggregate shape, the temperature and the concentration. Experimental observations performed by fluorescence quenching, NMR, and small angle scattering measurements [19] give an aggregation number N of ~60 for monovalent surfactant with 11 methylene groups in the alkyl chain and ~80 for divalent surfactant with 14 methylene groups. Typical surfactants from the first kind as SDS (sodium dodecylsulphate C12 SO 4 Na), can have the aggregation number between 50 and 100. The micellar aggregation is a dynamical process that supposes reversibility; each second, some 10^3 to 10^6 monomers are taking part to the aggregation and in the same time, about 0.1 to 10 2 micelles are breaking up.

Both processes rates are related to the CMC value and become faster as this one increases. The micelle lifetime is about 10^{-2} to 10 seconds [20]. Both local molecular dynamics (flexions, torsions, isomeric rotations) and surface diffusion effects are superposing. The density of the medium essentially governs fast motions, while slow motions are more related to the local structural parameters. Development of macroscopic investigations, such as conductivity measurements or infrared spectroscopy of water and polar head bonds, can help the interpretation of molecular dynamics.

Temperature also, must be taken into account for micelle aggregation, because it introduces a new condition: it has to be lower than a certain value, known as the "Point Krafft" (PK), listed in Table1.1 [21], together with the CMC values for various surfactants. In Table 1.1, substances in the first five lines are nonionic surfactants and in the last three lines are ionic surfactants; C_n represents the number of carbon atoms of the alkyl chain and EO_n represents the number of the ethylene oxide groups of the polar head.

Table1.1 Typical CMC values for some usual surfactants

Surfactant	Krafft temp. ˚C	CMC mol dm^{-3}
$C_8\ EO_6$	25	$9.9x10^{-3}$
$C_{10}\ EO_6$	20	$9.5x10^{-4}$
$C_{12}\ EO_6$	25	$6.8x10^{-5}$
$C_{12}\ EO_8$	25	$7.1x10^{-5}$
$C_{14}\ EO_8$	25	$9.0x10^{-6}$
$C_8\ SO_4\ Na$	25	$1.3x10^{-2}$
$C_{12}\ SO_4\ Na$	25	$8.3x10^{-3}$
$C_{16}\ SO_4\ Na$	25	$2.1x10^{-4}$

Remark that, the CMC values reduce by a factor of 10 for each addition of two CH_2 groups to the alkyl chain for nonionic surfactants and of four CH_2 groups to the alkyl chain for monovalent ionic surfactants.

The CMC was determined from conductivity and pH measurements and it has been found that it is considerably higher for bivalent ionic surfactants than for monovalent analogues containing the same number of methylene groups in the alkyl chain, probably $CMC =$ depending on the increasing electrostatic repulsion between the polar headgroups [22]. For charged surfactants, the electrostatic interactions are often the dominating factor in determining the properties of the systems. Comparison between monovalent and divalent amphiphilic molecules behavior in lyotropic solutions demonstrates that physicochemical differences become important.

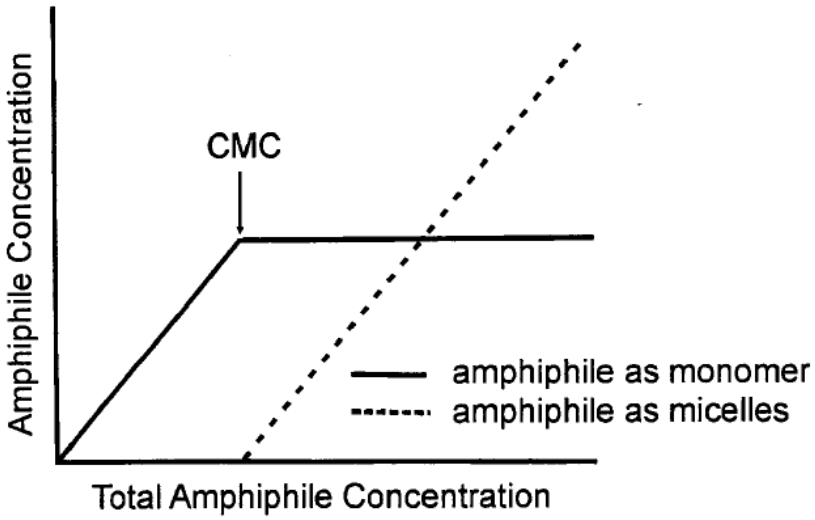

Figure. 1.5: Varions of CMC value.

Under the CMC value, some physical parameters such as density, electrical conductibility, osmotic pressure and boil temperature increase with concentration, but present suddenly a significant variation upon the CMC value, as in fig.1.5. At concentration higher than CMC value, most of the monomers form a film at the water surface till saturation. After that, a new equilibrium is established and the micellisation process generalizes in the bulk.

The amphiphilic molecules free energy [23] may decrease considerably by forming large aggregates (N>40). Chemical exchanges between monomers and micelles can be described by the chemical potential equilibrium:

$$\mu_1^0 + k_B \,\mathrm{Tln}\,\chi_1 = \mu_m^0 + \frac{k_B T}{N} \ln \frac{\chi_m}{N} \qquad (1)$$

Where μ_1^0 and μ_m^0 are chemical standard potentials for a free monomer and for a monomer in a micelle, respectively; χ_1 and χ_m are the molar fractions of monomers and micelles, respectively; the logarithmic terms are the entropies of the mixtures in water and in micelles and N is the aggregation number. Supposing N is constant and known, one can determine the molar fraction of the micelle and the CMC value by imposing the condition that the monomer concentration is maxima:

$$\mathrm{CMC} = \chi_1^{\max} = \exp\left[-\frac{\mu_1^0 - \mu_m^0}{k_B T}\right] \qquad (2)$$

The shape of the aggregates in isotropic micellar solutions is ordinary spherical (globular) as shown in Fig. 1.7.

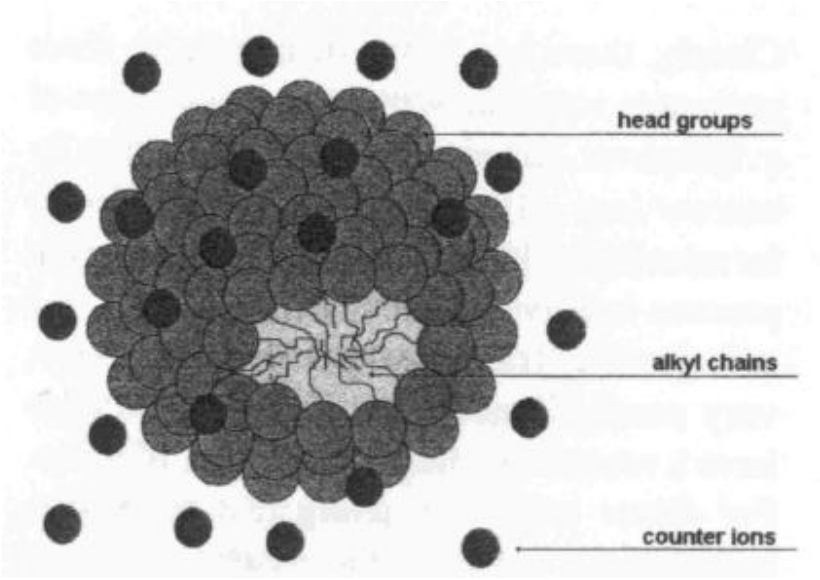

Figure: 1.6 – Formation of spherical micelle

In a mesomorphic state, aggregates can have different other shapes, such as cylindrical, rod-like or disc-like. In aqueous solutions micelles are called *normal*, meaning that the head of the amphiphilic molecules are in contact with water molecules, while the hydrocarbon tails entirely occupies the interior of the micelles. Below a certain specific water content which appears to be determined by the maximum capacity of the hydrophilic groups for binding water, the two parts of the amphiphilic molecule interchange position and micelles become *reversed*. The same molecular arrangement also occurs at any concentration in all the solutions with nonpolar solvents.

The aggregation shapes are submitted to a geometrical constraint; one of the three dimensions must be limited by the value *2l*, where *l* is the amphiphilic molecule length in complete extension. That is why, the most convenient shape is the spherical one, but also rods, lamellae

or discs are available. To classify and study those structures, the introduction of a packing parameter *P* is imposed:

$$P = \frac{v}{al} \qquad (3)$$

where *v* is the molecular volume and *a* is the medium area of the cross section of the polar head.

For an amphiphilic micelle with a spherical shape of radius *r*, the total micellar area *A* and the volume *V* are:

$$A = Na = 4\pi r^2 \quad \text{and} \quad V = Nv = \frac{4}{3}\pi r^3 \quad \text{hence} \quad a = 3\frac{v}{r} \qquad (4)$$

Making the same calculation for a cylindrical micelle of radius *r* or a lamellar one of width *2r* and ignoring the edge effect, the possible values of the medium area of the cross section of the polar head *a* and the packing parameter *P* are:

$$a \geq 3\frac{v}{r} \quad \text{and} \quad P < \frac{1}{3} \quad \text{for spherical aggregates (radius } r\text{)} \qquad (5)$$

$$a \geq 2\frac{v}{r} \quad \text{and} \quad P < \frac{1}{2} \quad \text{for cylindrical aggregates (radius } r\text{)} \qquad (6)$$

$$a \geq \frac{v}{r} \quad \text{and} \quad \frac{1}{2} < P < 1 \quad \text{for lamellae or discs (width } 2r\text{)} \qquad (7)$$

For molecules with a certain hydrocarbon chain length, the packing pattern strongly depends on the size of the polar head. All shapes just mentioned are possible if the values *a* are large enough; if not, only the disc shape is available. The great flexibility of the hydrocarbon chains make impossible the estimation of the smallest values for *r* which implies certain difficulties to precisely define the maximal values for *a*. Both theoretical and experimental observation [24] show that surfactants with the head composed by many groups regularly form spherical micelles, those composed by less groups form rods and those composed by

even less groups, form discs. At the CMC, the entropy favors the aggregation and smaller aggregates are preferred, i.e. spheres to rods and rods to discs.

The micellar aggregation is the result of a complex process, called *the hydrophobic effect*, which describes the interaction between nonpolar surfactants and water. It is well known that nonpolar surfactants are almost insoluble in water and generally have a very small degree of solubility. A thermodynamic analyze of the process shows that the immersion of hydrocarbon in water at room temperature, can be always associated to an increasing entropy, decreasing to zero enthalpy and a resulting high positive free energy. In a series of recent publications [25], this matter is discussed in detail. They consider the hydrophobic effect as a result of two contributions; the first one imposed by the surfactant ordering around water molecules and the second one imposed by the creation of a cavity in water, sufficiently large to include the nonpolar chains.

The first contribution is associated with negative entropy, because water molecules in the vicinity of a nonpolar compound have less possible configurations than the "free water" and are not able to built hydrogen bridges with the solute. The strong hydrogen bridges between water molecules themselves justify small values of the enthalpy. The second contribution is justified by the high energy required by the construction of the nonpolar cavity in the water. On one hand, the energy value is large because of the higher degree of cohesion between water molecules through the hydrogen bridges and on the other hand, because of the smaller dimension of water molecules in comparison with those of the surfactant. The strong bounding created by the hydrogen bridges that water provides, leads to a very high ordered aqueous structure.

The hydrophobic effect is very weak for nonpolar solutions, because of the repulsion that arises between water molecules and hydrocarbon or any other nonpolar groups. Otherwise, the ordering shall increase, reducing the entropy. The specific micelle shape closing inside the hydrocarbon tails of the amphiphilic molecules, favors the creation of a hydrocarbon zone, far from the water molecules. Hence, both thermodynamic conditions implied in the micellar stability are solved; the minimization of the hydrophobic interactions and the maximization of the hydrophilic interactions as well.

In aqueous solutions, the micellar surface is rather rough, because the heads of the amphiphilic molecules over cross the ideal geometrical micellar surface for about 0.2-0.5 nm. The existence of small volumes between the polar heads increases the possibility of counterions bounding. The number of counterions in the diffuse layer decreases because of

the very strong bounding between them and amphiphilic ions of the surfactant, which contribution to the micellar superficial potential is of a great importance. That distribution favors the sudden decrease of the molar conductance and of the electrical conductibility near the CMC value.

In nonpolar solvents, because of their small electrical permittivity, the micellar aggregation becomes more difficult. The interactions with the solvent are weaker and the micelle aggregation pattern is of the *reversed* type; the polar heads form the micellar core while the alkyl chains form the micellar surface contacting the nonpolar solvent. The polar core of the *reversed* micelles develops cohesion on the behalf of the dipolar bounding and the hydrogen bridges, in complete opposition with the hydrocarbon core of the *normal* micelles, where the mainly spherical shape supposes high osmotic pressure which confines the hydrocarbon tails and make them have different proprieties than the free surfactant molecules. In nonpolar solutions, the micellisation process does not begin at the CMC value but upper and the number of the micelles is rather smaller than the *normal* micelles formed in a polar solvent. The number of *reversed* micelles could increase only in the presence of small quantities of water to solve the bounding of the polar groups.

In conclusion, decreasing the surfactant concentration under CMC, leads to the micelle dissociation and the solution turns up to the initial isotropic liquid state. At CMC, micellar solutions appear, but they are not yet liquid crystals because of ordering absence; increasing concentration leads to the extension of the micellar ordering till completely ordered phases appear, which really means the liquid crystal state. Temperature constraints are also imposed.

1.7 Lyotropic ordering

In order to identify all the lyotropic phases, there are some important methods of investigation, such as polarized light microscopy, X-ray scattering and RMN spectroscopy. Here are the different phases revealed by these methods; lamellar *L*, cubic *I* or *V*, hexagonal *H*, nematic *N*, cholesteric *Ch* and some intermediate ones.

All of them, with one exception, are birefringent and present typical textures; the cubic phases are isotropic (like micellar solutions) so, they cannot be detected in polarized light investigation, but they have also a high viscosity, which make the difference. There is a particular phase, not yet mentioned named *gel*, where both the surfactant and the water have a very slow mobility, while mobility of all the other phases is high, like as liquids. Every phase distinguishes from another by the specific long distance symmetry of the arrangement of the

micellar aggregates and by the micellar surface curvature. Excepting the lamellar phase, with a planar molecular arrangement, all the other phases can be considered as continuous in the polar region, at least.

Lyotropic phases can be found in a *normal* or a *reversed* state and the index 1 or 2 respectively, will be attached to the appropriate phase symbol. One can found for the lyotropic phases, different other names belonging to the usual soap manufacture terms, due to the direct application of that kind of amphiphilic in practical life. By adding water to an amphiphilic crystal, the crystalline structure turns into a lamellar *normal* one, also called *neat soap*. If the water addition process continues, the cubic *normal* phase also called *viscous isotropic* appears followed by the hexagonal *normal* phase also called *middle soap* and then the micellar isotropic liquid state, presenting association micelles, is obtained. Not all amphiphilic surfactants have the same phase succession as presented here, but the hydration process always finalizes by the isotropic liquid state for all of them.

Amphiphilic aggregates are always associated in such a structure to fulfill the free energy minima. The main forces implied in these structures are electrostatic and dispersive. The dispersive are generally weak forces, but sometimes they may govern the ordering interactions between molecules. The electrostatic are attractive forces between ions or dipoles (ion-ion, dipole-dipole, and ion-dipole). Increasing temperature may destroy these arrangements. Depending on temperature and concentration, all lyotropic phases can occur in the same solution passing by multiple phase transitions.

In the next sections, the lyotropic ordering is discussed in two distinct parts; in the first one (1.8), the main characteristics of all mentioned phases are detailed, while in the second one (1.9), a supplementary phase typology is revealed by means of the multiple conformational states of the hydrocarbon chain, symbolized by α ,β ,β',δ ,$\alpha\beta$ and γ .

1.8 Specific structures

1.8.1 Lamellar structure – *Neat soap*

The structural unit for the lamellar phase is the simple and double layers. It has to be mentioned that the bilayer, as a repetitive unit, forms the main matrix of the biological membranes that contain phospholipids as lyotropic compounds and not soaps.

The ordered bilayer structure is formed by amphiphilic molecules disposed in bidimensional infinite layers, delimited by water layers, all of them having a parallel disposition. The ionic heads of the molecules are contacting the aqueous medium, while the hydrocarbon chains are

interdigitating in order to avoid water. The bilayers are disposed one under another through the third dimension, periodically alternating with water layers, like in fig.1.7 [26]. Because the bilayer ordering is not disturbed by the gravitational effect, the repetitive vertical distance between layers is constant. This phase is not a viscous one and the bilayers can slip easily one on the other. The specific optical characteristics of its textures make easier the identification of this phase.

The optical axis is parallel to the long axis of the molecules of the layers; the phase can be optically uniaxial, positive or negative, depending on the temperature values.

The usual investigation method for the lamellar phase is the X-ray scattering that gives the following results [27]: the width of the double layer is of 30-40 Å, smaller than the double of the amphiphilic molecule length; the width of the intercalated water layers is of about 20 Å. These figures vary with temperature and concentration in the limits of the lamellar phase. The hydrocarbon chain folding configuration or the tilt angle of the molecules in the layer determines the width variation.

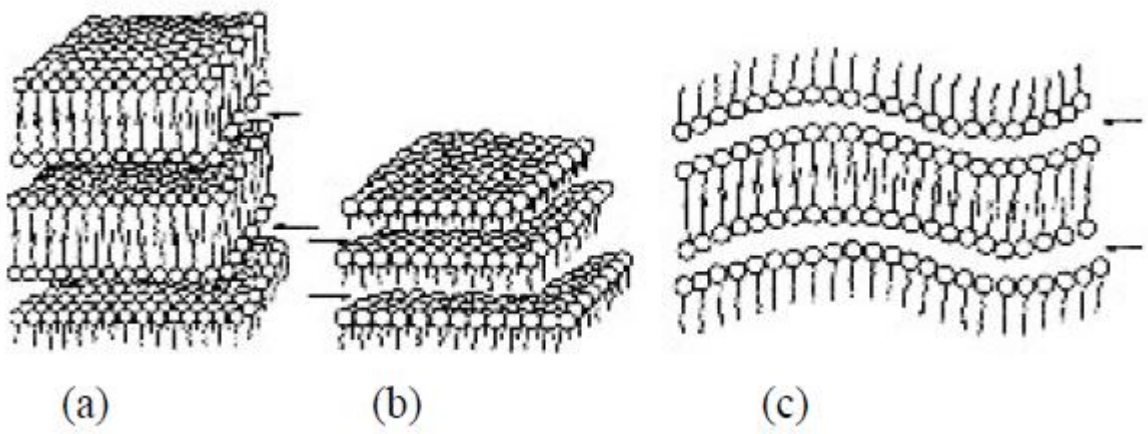

Figure:.1.7 Lamellar structure: (a) bilayer, (b) monolayer, (c) rippled bilayer; arrows indicate water layer location.

1.8.2 The Cubic Structure – *Viscous Isotropic*

As the name of the structure indicates, in that case, micelles arrange themselves in a cubic pattern and show always three different packing forms: cubic, cubic face centered and cubic body centered. There are two distinct micellar aggregation shapes: the first one is spherical and forms the *I* phase while the second one is rod-like, interconnected in a three dimensional scheme and form the *V* phase. Considering also the *normal* and the *reversed* arrangements in

both *I* and *V* phases, finely there are four different cubic structures in discussion. From an optical point of view, cubic phases present no texture, because they are isotropic and can be distinguished from the isotropic micellar solutions only by their high viscosity. The cubic phases *I* and *V* can be correctly identified one from another by their precise location among other phases. In the hypothesis of increasing progressively the surfactant concentration, the *I* phase location is between the isotropic micellar solution and the hexagonal one, while the *V* phase location is between the hexagonal phase and the lamellar one.

The *I* phase has the simplest configurations; all three mentioned packing forms are present for instance in the C_{12} EO_{12} /water solution in a *normal* I_1 arrangement. For that nonionic surfactant solution, a polyhedral representation in all three packing forms (see fig. 1.8) [28] has been appropriate.

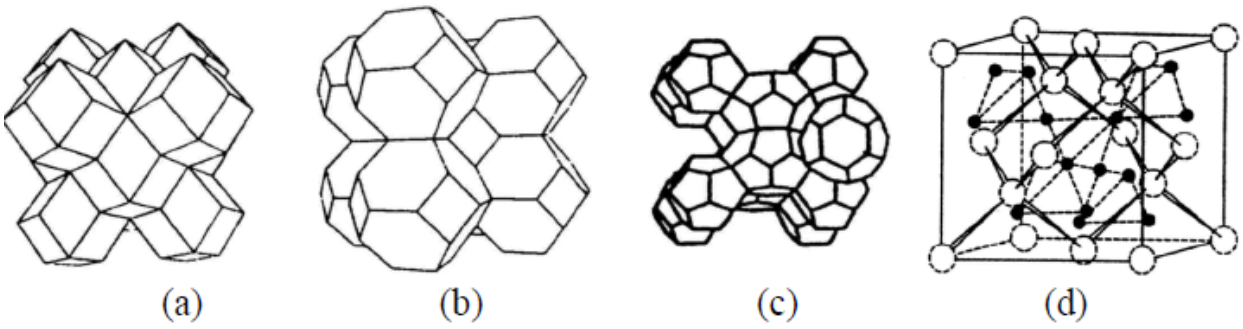

Figure: 1.8 - Cubic phases in a polyhedral micellar arrangement

Configuration (a) has been the subject of several hypotheses concluded as the following one: the polyhedral volume consists in two spherical micelles and six disc micelles. This packing network is convenient with the energetic stability condition too. Configurations (b) and (c) are very well described by considering identical micelles with quasispherical shape proposed by Seddon.

There are surfactants that form the cubic *I* phase in a *reversed* I_2 arrangement; micelles are supposed to be spherical, of two different sizes, disposed in the (d) configuration [29]. In all *reversed* structures, the packing constraint $r<l$ for spherical micelles, does not work anymore because of the external disposition of the hydrocarbon tails. That is why, two different micelle sizes are allowed to grow and to coexist in the same solution. In the *V* phase, the three-dimensional lattice consists of short rod-like micelles with the face curvature facing

water (V_1), or the nonpolar solvent (V_2) . They form three interesting bicontinous network (see fig. 1.9)

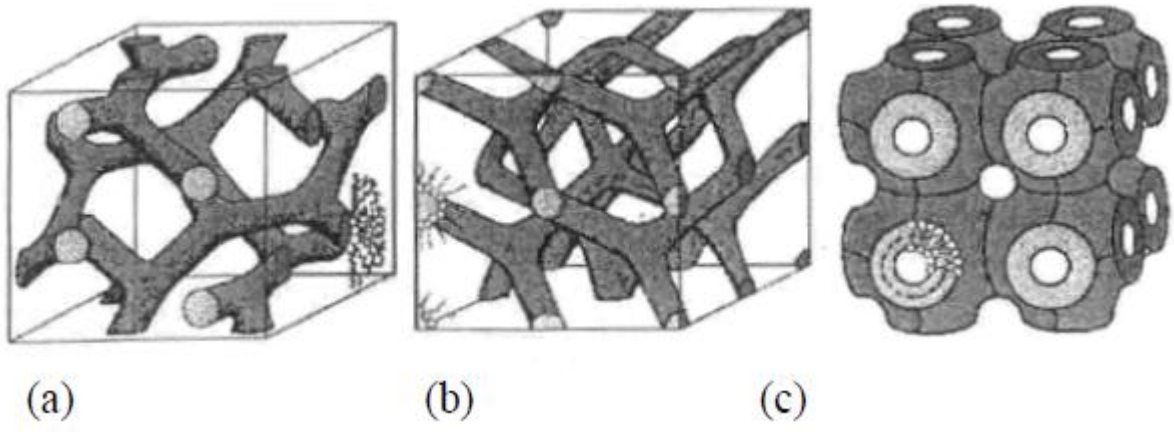

Figure:1.9 - Cubic phases with "bicontinous" structure

For the (a) network in Fig. 1.9, Luzatti [30] supposes that both surfactant and water form short cylinders that couple together three by three and form two independent interdigitating branches.

Luzatti and Tardieu [31] propose for the (b) network in fig.1.10, two tetrahedral interwoven ramifications arranged in a double diamond structure, and for the (c) network in fig.1.10, they propose long water cylinders joined six by six in a cubic pattern.

1.8.3 Hexagonal Structure – *Middle Soap*

If increasing solvent concentration in the cubic phase, the hexagonal phase occurs and forms *normal* structures H_1, or *reversed* structures H_2, according to the solvent polarity. Micelles are very long aggregates, rod-like, which can have circular, square, rectangular or hexagonal cross sections. These rod-like aggregates are the structural unit of that structure. With no respect to the continuous medium nature, rods disperse with their long axis in a parallel disposition, creating hexagonal, tetragonal or orthorhomboidal patterns.

The amphiphilic molecules arrangement is a radial one around the rod long axis, with the polar groups exposed to the exterior in the H_1 structure, or with the hydrophobic tails exposed to the exterior in the H_2 structure; the continuous medium is water and hydrocarbon, respectively. Both the *normal* and the *reversed* types are shown in fig.1.10.

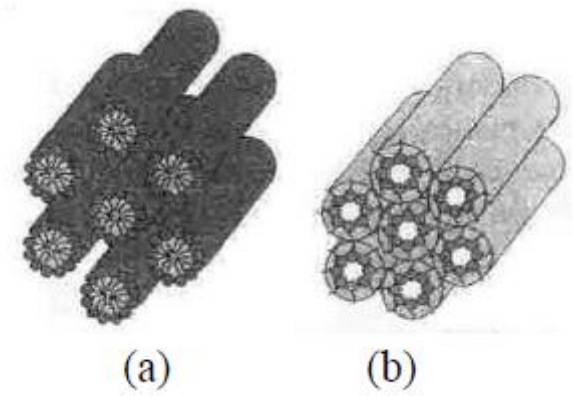

Figure: 1.10 - Schematic representation of a *norma*l (a) and *reversed* (b) hexagonal phase

Using X-ray scattering [34], it has been found that normal rods have a diameter of 1.3 to 2 bigger than the hydrophobic chain length. The dimension of the separation zone between rods is in the 0.8-3 nm ranges for the *reversed* type, and up to 5 nm for the *normal* type. Both types show similar optical textures and present a higher viscosity in the hexagonal phase than in the lamellar phase.

1.8.4 The Nematic Structure

Certain solutions of lyotropic surfactant present nematic structures, like thermotropic nematics, i.e. orienting themselves in external magnetic field or under mechanical stress and showing typical Schlieren textures when observed in polarized light. Lyonematic structures were discovered by Lawson and Flaut [32] by adding the corresponding alcohol to aqueous solutions of ionic surfactants with 8 and 10 carbon atoms of alkyl chain. Many ionic ternary solutions such as SDS/decanol/water, sodium decylsulphate (SdS)/decanol/water and potassium laurate (KL)/decanol/water, form nematic structures in a relatively narrow concentration/temperature range. Other ionic surfactants, as short chain fluorocarbon derivatives, show nematic phases in binary structures with water. The most extensively investigated example of these compounds is the cesium per-fluoro-octanoate (CsPFO). An example of nonionic surfactant that forms a nematic structure in a binary aqueous solution is the C_{16} EO_8. Recently it was shown [36] that other nonionic surfactants, such as hexapolyethilenoxi triphenil derivatives, present lyonematic phases.

Aggregates in the nematic phase are finite and anisotropic; due to the one-dimensional ordering characterized by the director n, and presents an important translational disorder. There are two different micelle shapes in nematics, as in Fig. 1.12.

Concluding the experimental observations, three types of nematic phases are implied: the nematic discotic phase N*d*, the nematic calamitic phase N*c* and the nematic biaxial phase N*bx* . Both N*d* and N*c* phases are optically uniaxial and the oriented samples investigations revealed that N*d* is uniaxial positive and N*c* is uniaxial negative [37]. The discotic phase is formed by planar disc micelles and is related more to the lamellar phase, because micelles are built like *rounded bricks* or *ruler shaped,* rather than circular discs. The calamitic phase is formed by rod-like short micelles, and is related to the hexagonal phase.

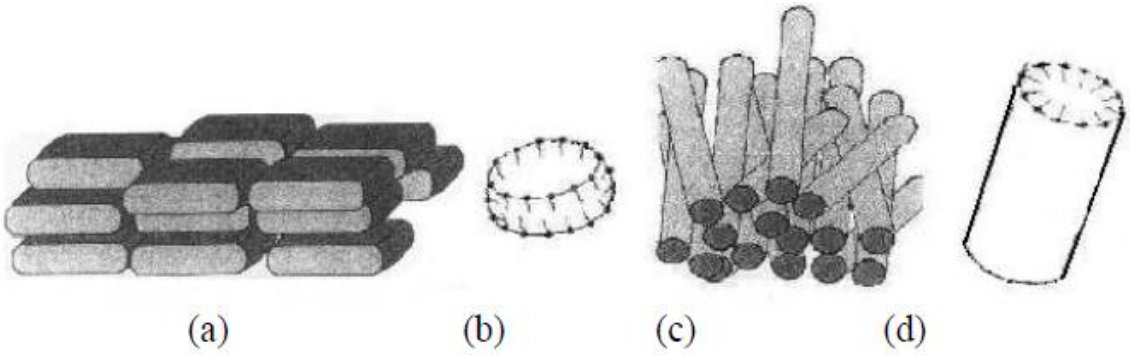

Figure. 1.11 - Representation of nematic phases: (a) discotic micelles like rounded bricks; (b) cross section in a discotic micelle showing amphiphilic molecules distribution; (c) rod-like calamitic micelles; (d) cross section in cylindrical micelle showing amphiphilic molecules distribution

In a concentration/temperature representation, the biaxial nematic phase always occurs between N*d* and N*c* phases. By consequence, some authors are presenting it as a mixture of the two types of micelles found in that ones. The N*bx* phase has been found by Yu and Saupe [38] in the ternary solution KL/decanol/water in a narrow temperature domain at a constant decanol concentration of 6.24% and has been studied in detail by Galerne *et al.* [39]. According to experimental observations, it has been found that the following five lyonematic solutions only, present all three nematic phases:

- Potassium laurate/decanol/water [40]
- Sodium decylsulphate/decanol/water [41]

- Potassium laurate/decylammonium chloride/water [42]
- Sodium decylsulphate/decanol/water/sodium sulphate
- Sodium dodecylsulphate/decanol/water

The microscopy in polarized light shows typical nematic Shlieren textures; a planar texture for the N*c* phase (as a monocrystal cut parallel to the optical axis) and a homotropic texture for the N*d* phase (as a monocrystal cut perpendicular to the optical axis). In order to improve the understanding and study of the nematic textures and their dependence on concentration, Neto *et al.* [43] proposes the *gradient concentration method* that better indicates the phase succession. Lyotropic nematic structures are located between the well ordered phases (lamellar, cubic, hexagonal) and the completely disordered phases (micellar isotropic solutions). Recently, the N*c* phase of the KL/decanol/water solution was X-ray investigated and it has been found that the micelle section is elliptical instead of being circular, as the random distribution of potassium laurate and decanol molecules around the micelle long axis, indicates.

Literature review

Shukla et al.[34] describe the morphological, thermal and chemical evaluation of cationic surfactant, cetyl prydinium chloride ($C_{21}H_{38}NCl$) with increasing concentration in polar solvent, ethylene glycol $C_2H_4(OH)_2$ exhibiting the lyotropic liquid crystal behavior. Results indicate the existence of the mixed lyotropic liquid crystalline phase in these systems at lower concentration and single phase at intermediate concentrations.

Caiqi Wang et al.[35] reported that the lyotropic liquid-crystalline behavior of trimethylsilyl hydroxypropylcellulose (TMS-HPC). The introduction of the trimethylsilyl (TMS) group in the parent HPC increases the solubility in organic solvents, and the lyotropic mesophase can be formed in concentrated acetone solution. The critical concentration (C*) in acetone is approximately 36%. The liquid crystalline nature of TMS-HPC/acetone solution was confirmed by PLM, and the mechanism of liquid crystallization was studied by FTIR and WAXD methods.

Wilson Quevedo et al.[36] reaveled that soft X-ray time-resolved scattering experiments with nanosecond time resolution (10 ns) and nanometer spatial resolution were carried out at a table top soft X-ray plasma source (2.2–5.2 nm). The investigated system was the lyotropic liquid Crystal C16E7/paraffin/glycerol/formamide/IR 5. Usually, major changes in physical, chemical, and/or optical properties of the sample occur as a result of structural changes and shrinking morphology. Here, these effects occur as a consequence of the energy absorption in

the sample upon optical laser excitation in the IR regime. The liquid crystal shows changes in the structural response within few hundred nanoseconds showing a time decay of 182 ns. A decrease of the Bragg peak diffracted intensity of 30% and a coherent macroscopic movement of the Bragg reflection are found as a response to the optical pump. The Bragg reflection movement is established to be isotropic and diffusion controlled (1 μs). Structural processes are analyzed in the Patterson analysis framework of the time-varying diffraction peaks revealing that the inter-lamellar distance increases by 2.7 Å resulting in an elongation of the coherently expanding lamella crystallite.

Pieranski.P et al.[37] shows that mono crystals of the cubic lyotropic liquid crystal phase V_1 are studied in droplets of the mixture C12EO6/water surrounded by water vapor of controlled pressure *p*. Shapes of mono crystals are found to depend on the conditions of growth from the lamellar phase and on the nature of the substrate. After the growth, when the lamellar phase is exhausted and crystals are in equilibrium with water vapors, their shapes are shown to depend on the pressure *p*.

Ali khana et al.[38] reported that mixed surfactant systems have been, for a long time, one of the favorite areas for experimental studies on interfacial and bulk properties of surfactants. Beyond the well-known synergistic properties, with relevance to technical applications, recent studies increasingly focus on the bulk aggregation behavior. As more systematic and detailed experimental data is collected (for example, by use of scattering and direct imaging techniques), increasingly refined theoretical models are developed. Most references reviewed here clearly show both the trends. Topics such as micellar growth, micelle-to-vesicle transition and equilibrium vesicle formation in dilute systems (in particular in catanionic systems) continue to expand and sometimes pose challenges to conventional notions of surfactant self-organization. As the rich polymorphism of mixed aggregates is unraveled, the possibilities of using them for broader goals also increase.

Hironobu Kunieda et al[39] concluded that phase diagram of a water-poly(oxyethylene) oleyl ether (POlE) system was constructed as a function of poly(oxyethylene) chain length at 25 °C. The POlEs contain a highly pure oleyl group, whose purity is above 99.7%. The POlEs are in a liquid state over a wide range of composition. The increase in the poly-(oxyethylene) (EO) chain of POlE corresponds to the increase in the curvature of surfactant layer toward water or the increase in HLB (hydrophile-lipophile balance) number of the surfactant. Various self-organizing structures were found: hexagonal and lamellar lquid crystals, four kinds of isotropic liquid crystals, a sponge phase, and reverse hexagonal liquid

crystal. The phase transition between normal hexagonal and lamellar liquid crystals were investigated at constant volume fraction of the oleyl group in system by means of smallangle X-ray scattering.

X. Auvray et al.[40] explains the method for the analysis of the phase diagrams of lyotropic compounds was employed to study the formation of liquid crystala from two surfactants, cetyltrimethylammonium bromide (CTAB) and cetylpyridinium bromide (CPBr) in water. Studies were also carried out in the protic solvents, glycerol (G), formamide (FA), ethylene glycol (EG), and N-methylformamide (NMF), and the aprotic solvents, dimethylformamide (DMF) and N-methylsydnone (NMS). Wile the normal succession of ordered phases appeared to be governed by geometric constraints of interface curvature, the differences in behavior were accounted for by the differences in cohesion energy of the solvents and the different natures of the polar heads of the two surfactants. In DMF**,** a solvent with low cohesion energy, both surfactants showed only lamellar phases, whereas CPBr with a highly delocalized charge on the polar head displayed a succession of conventional phases in all the other solvents. CTAB with a localized charge formed only lamellar phases in NMF and NMS**.** This behavior was interpreted a resulting from headgroup solvation due to dipoledipole interactions or hydrogen bonding. The particular case of NMS was accounted for by better stacking between the planar molecules of this solvent and the pyridinium rings of CPBr.

Tetsuro Iwanaga et al.[41] reported that effect of added salts (NaCl, Na2SO4, and NaSCN) or polyols (glycerin, 1,3-butanediol, ethylene glycol, and poly(ethylene glycol) 400) on liquid crystalline structures of polyoxyethylene-type nonionic surfactants was investigated by means of small-angle X-ray scattering (SAXS). The effective cross-sectional areas of the lipophilic parts of aggregates, *a*s, in both hexagonal and lamellar phases decreases upon addition of salts, which lower a cloud point in a dilute aqueous nonionic surfactant solutions. On the other hand, if added salt raises the cloud point, the *a*s increases. The similar results were obtained in the case of adding polyols. Since the *a*s mainly depends on the EO-chain length, the above results are the direct bevidence that the hydration or dehydration of the EO-chain is affected by these additives which causes the change in the *a*s in surfactant self-organizing structures. The effect of polyols on the three-phase behavior in water/heptaethylene glycol dodecyl ether (C12EO7)/heptane system was also investigated. Since 1,3-butanediol largely affects the HLB temperature, a considerable amount of the 1,3-butanediol is incorporated in the surfactant aggregates whereas the three-phase temperature is

almost unchanged in ethylene glycol and poly(ethylene glycol) 400 systems. Hence, it is considered that the *a*s value in 1,3-butanediol system is less accurate than those in ethylene glycol and poly(ethylene glycol) 400 systems.

Chapter 2
Methodology

2.1 Materials

In the present work, Cetyl perydinium chloride [($C_{21}H_{38}NCl$) Merk, 99% purity], N-Cetyl-NNN, Trimethyl ammonium bromide [($C_{19}H_{42}BrN$) Merk, 99% purity], Sodium dodecyl Sulphate [($C_{12}H_{25}SO_4Na$) Merk, 99% purity], protic solvent ethylene glycol [EG] (SD Fine chemicals, 99% purity) and silicon dioxide nano particles [(SiO2) Aldrich] particle size 5-15 nm were used as received.

2.2 Experimental

The binary mixture (CPCL:EG) was prepared by dissolving appropriate amount of CpCL in the ethylene glycol (40:60wt%) through various heatin and cooling cycles between melting and room temperature followed by sonication (37KHz) for 1hour near melting point of surfactant materials to ensure the homogeneity.

Non-aqueous binary mixture of CpCl:EG were prepared by desolving the appropriate amount of CpCl in ethy glycol along with the varying concentration of sio2 (0.05, 0.1, 0.5wt%). The resulting mixture were homogenized by heating the sample to its melting point in a sealed glass Vial followed by the sonication for 1hour at elevated temperature.

The prepared samples were filled between cleaned glass slides and then placed in a temperature controlled hot stage (Linkam TP 94 and THMS 600) with in ±0.10C temperature precision fitted on the polarizing microscope (Olympus BX-51P) stage. X-ray diffraction (XRD) patterns of the soft matter samples were scanned by diffractogram (Philips XPERT-PRO MPD) using Cu kα radiation source and patterns were recorded at 2θ = 1-10 range. The dielectric behaviour of these systems has been evaluated by RCL meter (Fluke model PM 6306) in the 50Hz-1MHz frequency span. Fourier Transform Infrared Spectroscopy (FTIR) is based on the fundamental principles of molecular spectroscopy.

2.3 Preparation of sample cells

The empty sample cells were prepared using conducting indium tin oxide (ITO) coated glass substrates. Glass substrates were procured from Bharat Electronics Limited (BEL), Bangalore. Some commercial cells obtained from M/S Linkam Instruments, UK were also used in the experiment with resistivity of the order of few 140-180 ohm-m. The substrates were initially washed with soap solution, rinsed with acetone (purity 99.9%), distilled water and then dried in a vacuum chamber. These ITO coated glass substrates were highly transparent.

The conducting sides of these ITO coated glass substrates were joined together and separation between the substrates was maintained with the help of mylar spacer of different thickness (μm). These two glass plates were sealed with optical adhesive. The electrodes were connected at the ITO coated substrate surface of the cell using indium (metal) ingot to obtaining better contact.

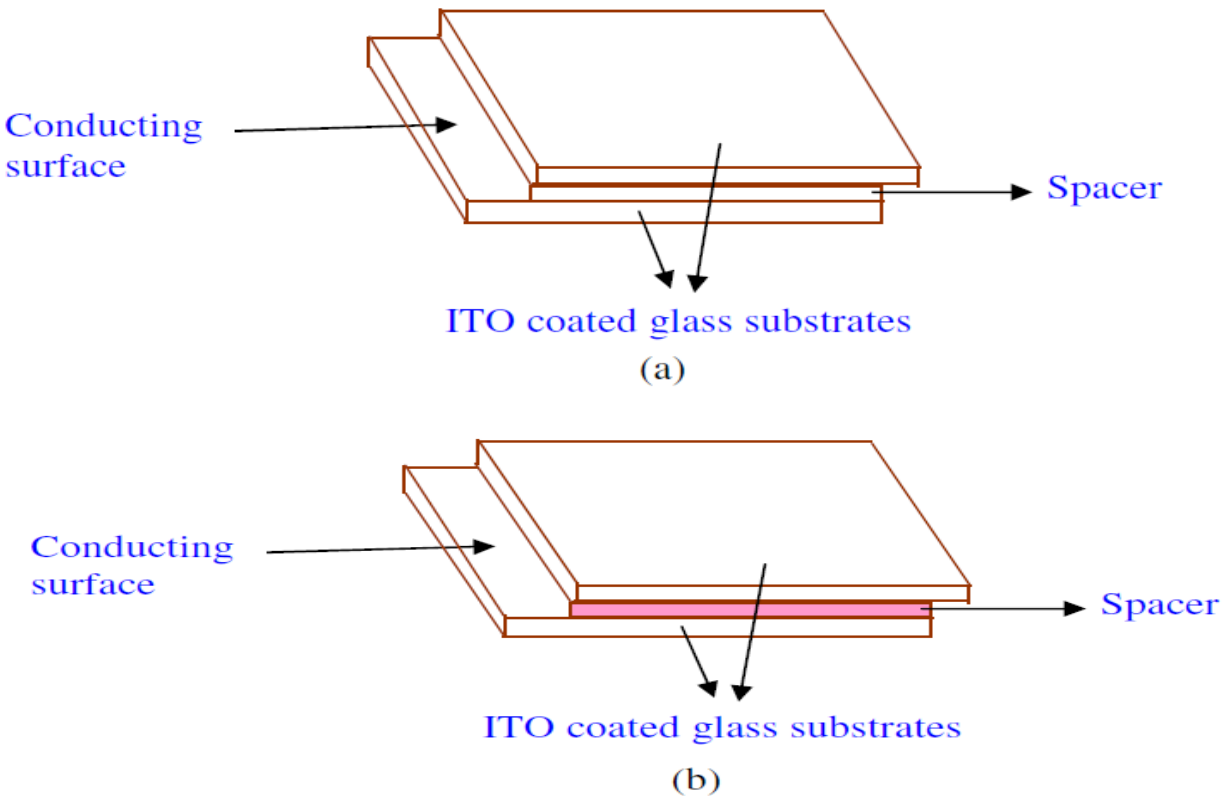

Figure.2.1 An assembled (a) empty (b) filled liquid crystal cells

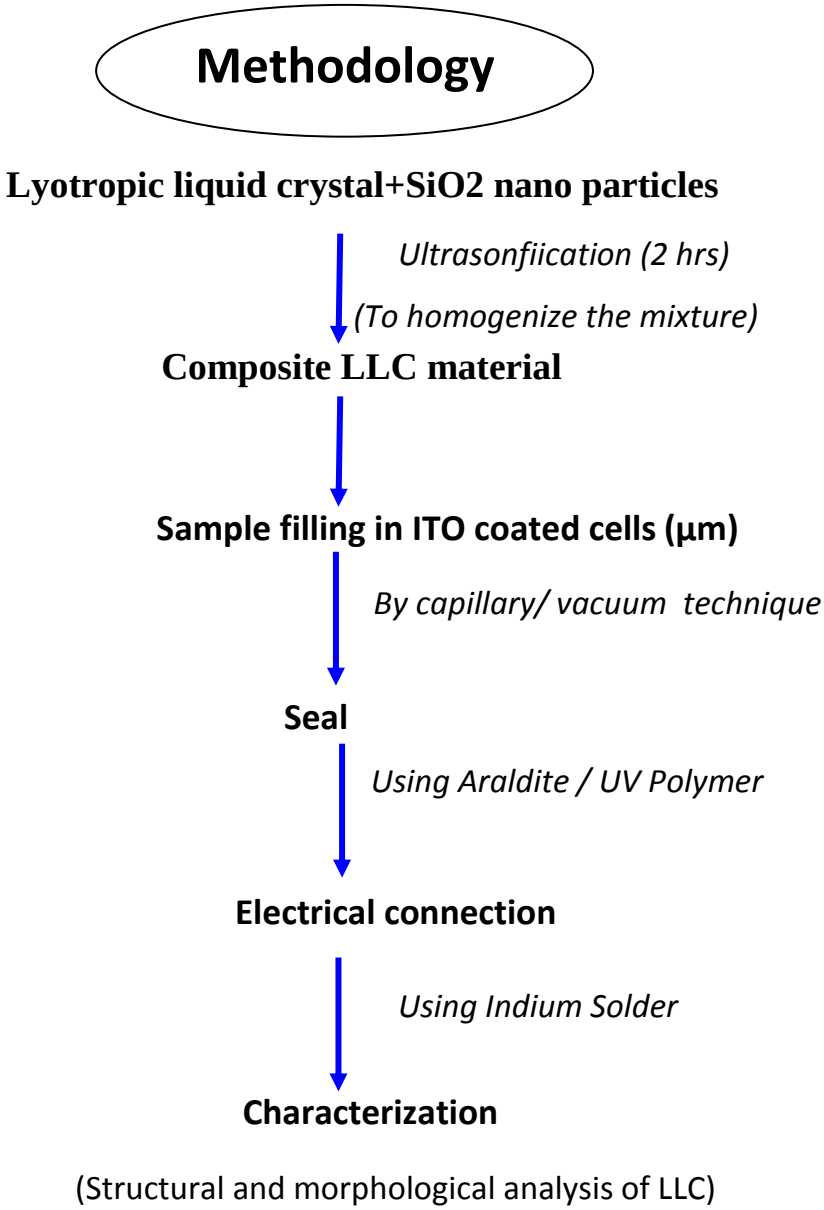

Figure.2.2 A flow chart for the preparation of SiO_2 nano partcles dispersed lyotropic LC samples.

2.4 Experimental technique

In order to study the liquid crystal morphology and phase transition temperatures, Olympus polarizing microscope (Model- BX51P) and Linkam temperature programmer cum hot stage (Model TP94 and THMS 600) were used. The electric field was applied to the sample through Scientech function generator (Model ST 4060), Philips function generator (Model FG8002). The microscopic optical textures were captured through the charge coupling device

(CCD) digital camera (Olympus DP 12 JAPAN) fitted on polarizing microscope and interfaced to a computer. A block diagram of our experimental set-up for the investigation of optical textures, electro-optic properties and other parameters of liquid crystal is shown in Fig. 2.3. The temperature of the SiO_2 nano particles dispersed LLC sample cell was controlled using temperature controller interfaced with computer through RS232 port and the output response as a function of field was recorded on a Tektronix Oscilloscope (Model TDS2024). Uniform dispersion of SiO_2 nano particles in the LLC and all the optical textures were viewed under crossed polarizer at a total magnification of 100X and 500X in the transmission mode. The complete experimental set-up to study morphological properties is also shown in Fig. 2.3.

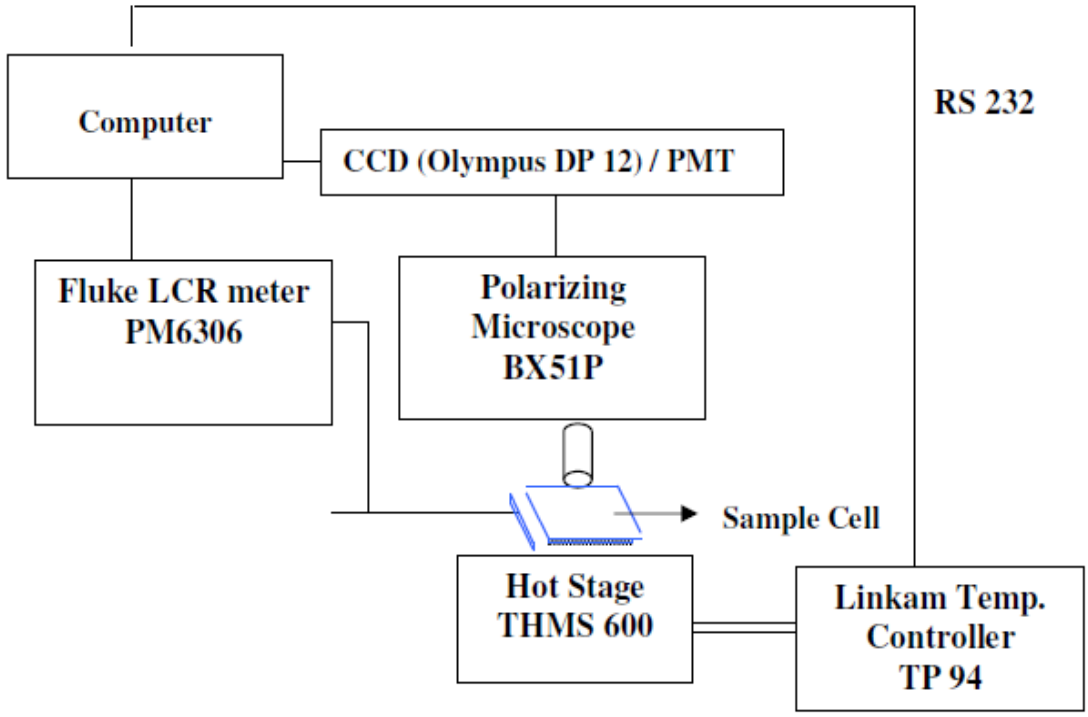

Figure. 2.3 Block diagram of the experimental set-up to study dielectric properties.

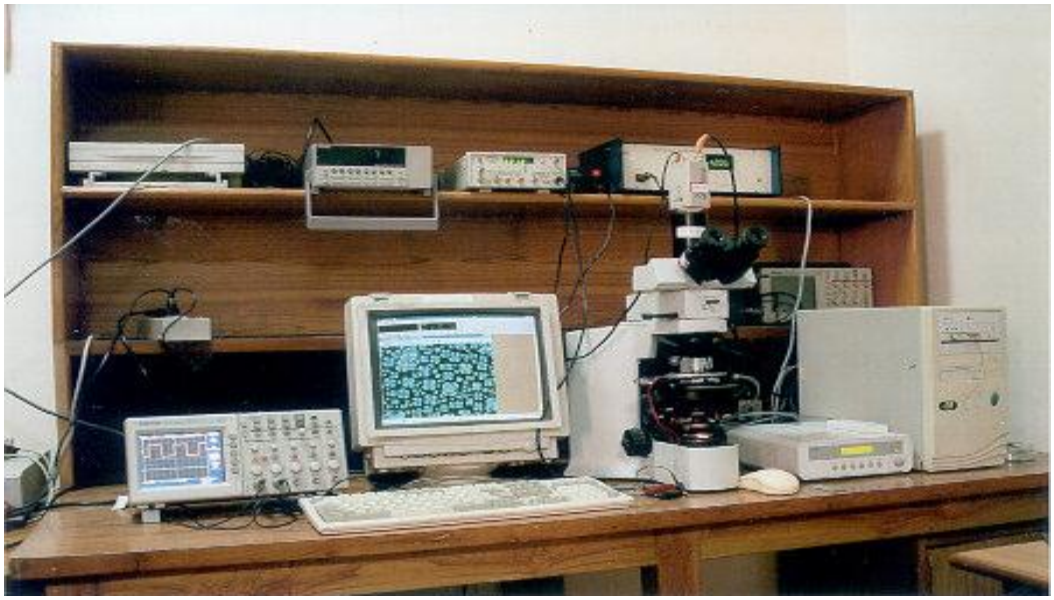

Figure. 2.4 Experimental set-up in the lab to study the morphological and dielectric studies of SiO_2 nano particle dispersed LLC films.

2.4.1 Optical polarizing microscopy

The optical studies observed in lyotropic liquid crystal and silica dispersed lyotropic liquid crystals were investigated using an Olympus optical polarizing microscope (Model BX51P) at a magnification of 100X under crossed polarizers using long working distance objective lens. The optical micro-textures of LC materials were also investigated as a function of temperature, voltage and other physical parameters.

2.4.2 Temperature programmer along with hot stage

In thermal microscopy studies, we used Linkam temperature programmer TP94 and hot stage THMS 600. The TP94 is specifically designed for precise temperature control of the Linkam heating/freezing stages. The stage sensor is digitally linearized to give accurate temperature readout, the controls and their functions have been carefully chosen for simple and easy operation. The temperature range is –196 ^{o}C to 600 ^{o}C. Heating or cooling rates can be changed almost instantly using the three rate keys. The heat ranges are from 0.1 to 0.9^{o}C/min at 0.1 degree intervals from 1.0 to 9.0 ^{o}C/min at 1.0 degree intervals and from 10 to 90^{o}C degree intervals. A varying dc signal is used to control the stage and results in an even application of power, which avoids the bursts seen with conventional burst fire ac techniques.

An optional remote control gives single key control of three programmable heating/cooling rates and the HEAT, COOL and HOLD functions. The three programmable heating/cooling rates are held in memory when power is switched off. The temperature and limit values can also be stored and recalled using the remote control facility.

2.4.3 Dielectric measurements

The dielectric measurements were carried out using a programmable automatic RCL meter (FLUKE PM 6306) in the frequency range 50Hz to 1MHz. The cell was calibrated using air and benzene as standard references. The frequency and bias dependence of the real and imaginary parts of the complex dielectric permittivity have been studied in detailed at room temperature. The dielectric properties of the SiO2 dispersed LLC were made in the presence of applied voltages that produced alignment (and, therefore, optical switching) of the LC phase. Dipole relaxation and ion-conduction-related processes were observed for samples. The dielectric behavior gave information on the reorientational motions of dipoles and the conduction behavior of extrinsic ions in the samples.

Figure. 2.5 Programmable automatic RCL meter [FLUKE PM6306] used for dielectric studies.

Dielectric spectroscopy technique measures the dielectric properties of a medium as a function of frequency. In the case of polymeric medium, dielectric spectroscopy is a powerful technique that is capable of probing the molecular motion and the electric properties. The dielectric constant or relative permittivity of a material is the ratio of the dielectric constant of

the material to that of vacuum. The capacitance measures the extent to which charge can be stored.

$$\varepsilon_r = \frac{\varepsilon'}{\varepsilon_o} \qquad (2.1)$$

The complex dielectric properties, the relative permittivity (Ɛ') and the loss factor (Ɛ") are determined by scans as a function of frequency and temperature. The displacement of the charge by applying the electric field is called "polarization". The dielectric properties of a material are defined by a complex dielectric permittivity,Ɛ*

$$\varepsilon^* = \varepsilon' - i\varepsilon'' \qquad (2.2)$$

Where ε' is the dielectric constant of the material, also known as the relative dielectric permittivity, and it is used to define the ability of the material to store electrical charge. Ɛ" is the imaginary part, which is related to the material loss and known as the dielectric loss.

2.4.4 Fourier transformation IR spectroscopy

FT-IR stands for Fourier Transform Infrared, the preferred method of infrared spectroscopy. FTIR is an analytical technique used to identify organic (in some cases inorganic) materials. This technique measures the absorption of infrared radiation by the sample material versus wavelength. The infrared absorption bands identify molecular components and structures. IR radiation is passed through a sample. Some of the infrared radiation is absorbed by the sample and some of it is passed through (transmitted). When a material is irradiated with infrared radiations, absorbed IR radiation usually excites molecules into a higher vibrational state. The wavelength light absorbed by a particular molecule is a function of the energy difference between the at-rest and excited vibrational states. The wavelengths that are absorbed by the sample are characteristic of its molecular structure. This makes infrared spectroscopy useful for several types of analysis

Figure.2.6 Fourier transforms infrared spectrometer (FTIR).

Typical applications

- Identification of foreign materials
- Particulates
- Fibers
- Residues
- Identification of bulk material compounds
- Identification of constituents in multilayered materials
- It can determine the amount of components in a mixture

2.4.5 X-Ray Diffraction

An x-ray diffraction technique is a non-destructive analytical technique, which reveals information about the crystallographic structure, chemical composition, and physical properties of materials and thin films. These techniques are based on observing the scattered intensity of an X-ray beam hitting a sample as a function of incident and scattered angle, polarization, and wavelength or energy.

Figure.2.7 X- ray Diffractometer

X-ray diffraction (Panalytical X'Pert) is an experimental technique that exploits the fact that x-rays are diffracted by crystals. X-rays have the proper wavelength (in the Angstrom range, ~ 10^{-8} cm) to be scattered by the electron cloud of an atom of comparable size. Based on the diffraction pattern obtained from X-ray scattering of the periodic assembly of molecules or atoms in the crystal, the density can be reconstructed. Additional phase information must be extracted either from the diffraction data.

CHAPTER 3

Result and discussion

This chapter summarize the results obtain from the various characterization to understand the morphological structural dielectric and chemical behavior of binary and ternary non-aqueous LLC mixture in the presence of varying concentrations of the SiO_2 nano particles.

4.1 Morphological and structural analysis

We have synthesized three systems (cationic, anionic, and nonionic) dispersed with SiO_2 nano particle. Optical texture of the as prepared, quenched, nano particle dispersed non-aqueous binary mixtures (x= pure, 0.05, 0.1, 0.5wt %) recorded at room temperature are shown in figure 4.1(a). The addition of surfactant molecules in the non aqueous medium shows some specific geometry after dispersing amphiphilic molecules in the solvent channels. CPCL: EG (40:60 wt %) binary phase have lamellar layered structure. It was found that after dispersion silica nano particle in the CPCL:EG system, the lamellar phase was not disturbed as we observed well defined fan like structure at all concentration as evident from figure 4.1(a).

Similarly in CTAB:EG system we observed fan like textures corresponding to the lamellar phase or hexagonal phase. It seems that the silica particles adjust themselves in the interstitial position between the layers. The textures shown in figure 4.1 (c) corresponding to the SDS:EG system. The texture observed are not much clear some fan like geometries are appeared which may be signature of hexagonal and lamellar phase, further confirmed via XRD analysis.

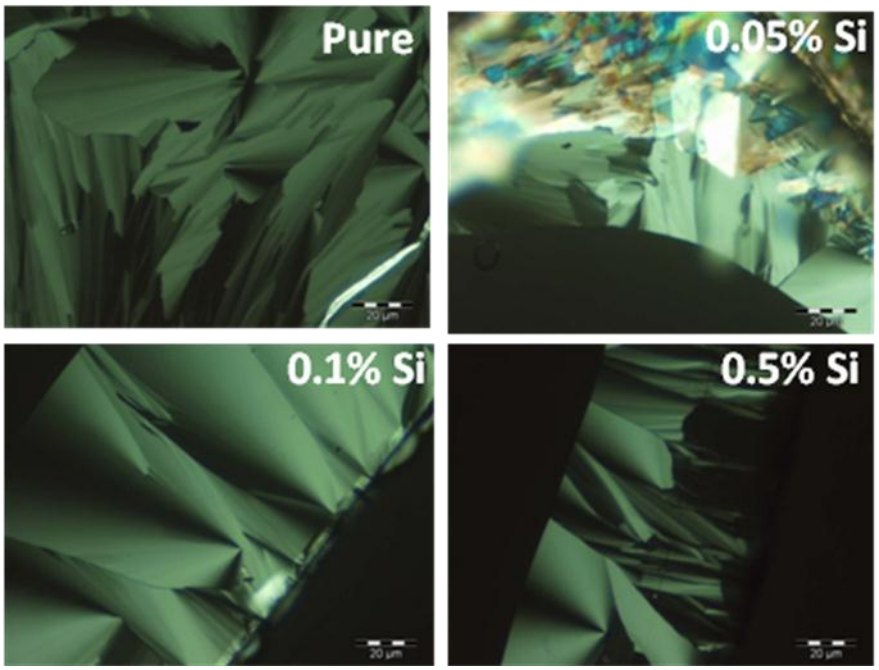

Figure 4.1(a): The texture morphology CPCL:EG:Si systems at 100X

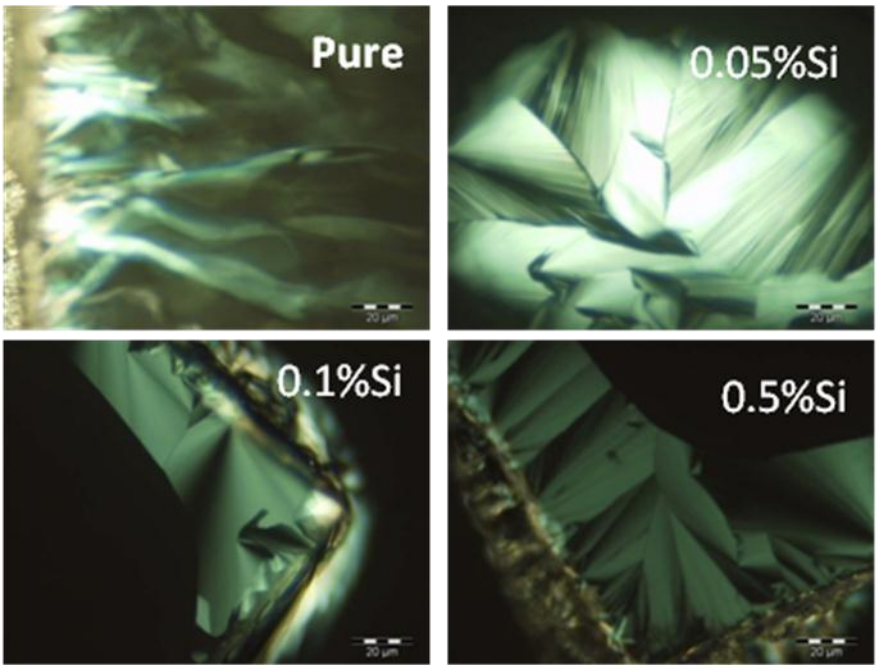

Figure 4.2(b): The texture morphology CTAB:EG:Si systems at 100X

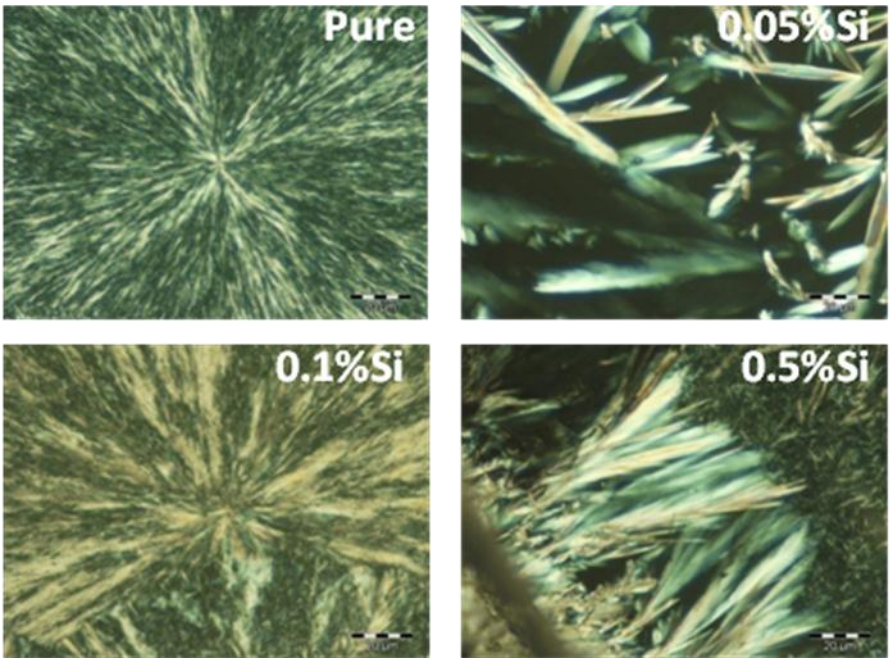

Figure 4.3(c): The texture morphology CPCL:EG:Si systems at 100X

4.2 Structural analysis by X-ray diffraction method

Wide angle X-ray diffraction was (At low angle) was used to identify the liquid crystalline phase of pure and dispersed system. Figure 4.2 (a) Shows the XRD pattern of the CPCL:EG:Si system.

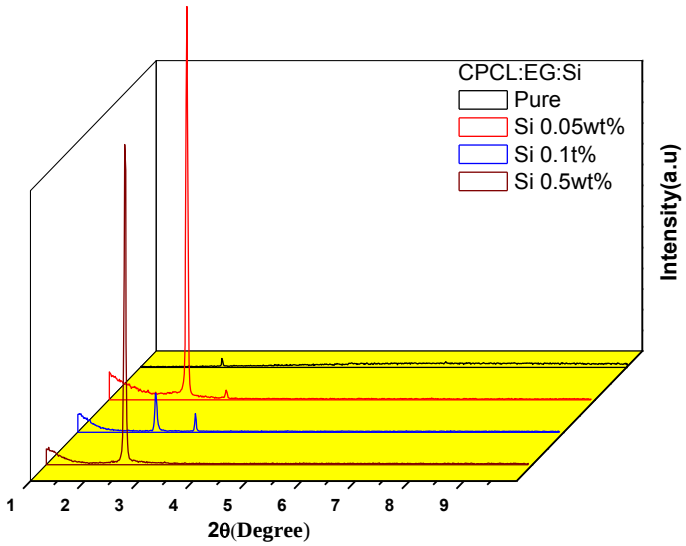

Figure 4.2(a) X-ray diffraction patterns of CPCL:EG:Si systems

In as pure system peaks observed are in 1:2 ratio, which are characteristics reflection of

lamellar mesophases. Si dispersed systems (0.05,0.1 and 0.5wt%) also displayed the reflection at same 2θ position are in 1:2 ratio corresponding to lamellar phase.

Figure 4.2(b) shows the XRD pattern of the CTAB:EG system. It was observed that pure system displayed for lines which are in 1:2:3:6 ratios matched as a lamellar mesophase. Sample contained 0.05 and 0.1wt% SiO_2 particle also displayed characteristics peaks which are in 1:2:6 ratios confining the lamellar phase. However at higher concentration 0.5wt% we observed four peaks which are in 1:√3:√4:√7 ratios characteristics of the hexagonal mesophase.

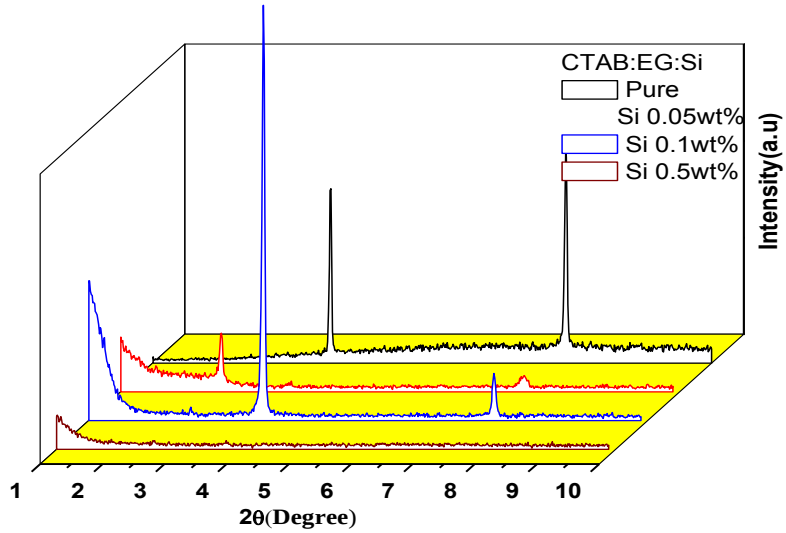

Figure 4.2(b) X-ray diffraction patterns of CTAB:EG:Si systems

The figure 4.2(c) presents XRD pattern of Si dispersed SDS:EG system. In pure SDS:EG system, peaks observed are in ratios, 1:√2:√3:√4 characterized as reflection of hexagonal phase. All the dispersed systems also show the same reflection corresponding to the hexagonal phase. However one unmatched peak observed in all concentration (2θ=1.8).

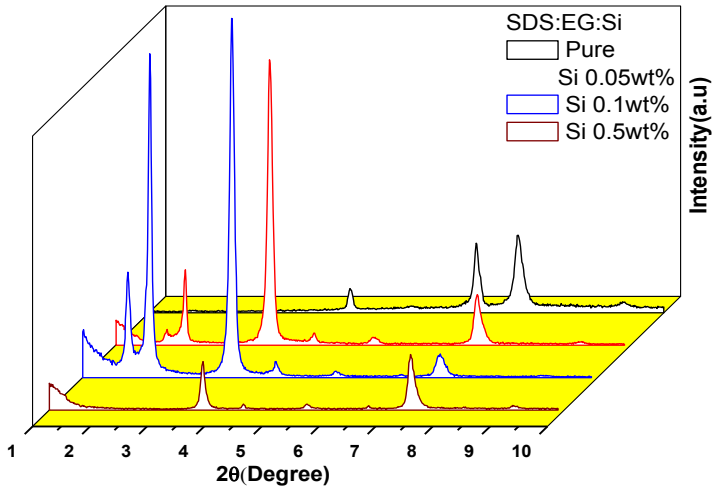

Figure 4.2(c) X-ray diffraction pattern of SDS:EG: Si systems

4.3 Dielectric spectroscopy

The temperature and frequency dependent dielectric behaviour of pure LLC phase and silica nano particle dispersed LLC phase was observed in the frequency range 50Hz to 1MHz.

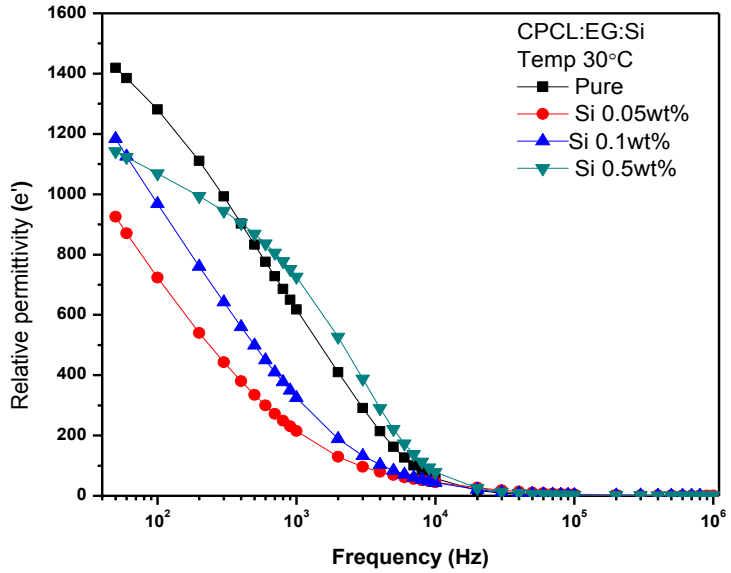

Figure 4.3(a) Variation of relative permittivity with frequency for CPCL:EG:Si systems room temp.

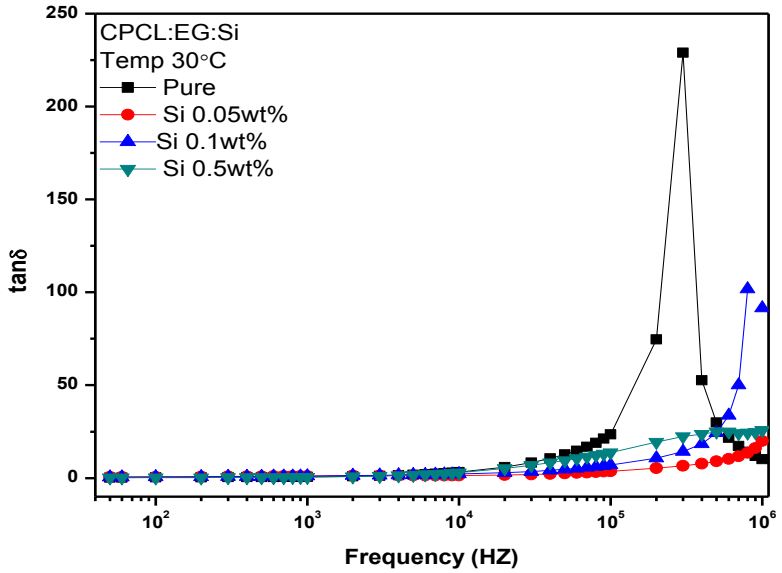

Figure 4.3(b) Variation of tanδ with frequency for CPCL:EG:Si systems room temp.

4.3.1: Dielectric study of CPCL:EG:Si systems

The variation in relative permittivity (**ε'**) as function of frequency for pure, CPCL:EG and silica nano particle dispersed samples are shown in figure 4.3(a) We observed that the pure

phase of CPCL:EG, system shows higher relative permittivity and attain maxima (1416) in the lower frequency region. It was seen that relative permittivity decreased with the addition of Si nano particles, which further increased with Si concentration though magnitude is less than that of pure system.

Figure 4.3(b) shows that tanδ v/s frequency plot. It was found that loss is minimum at lower frequency and increased at higher frequency zone.

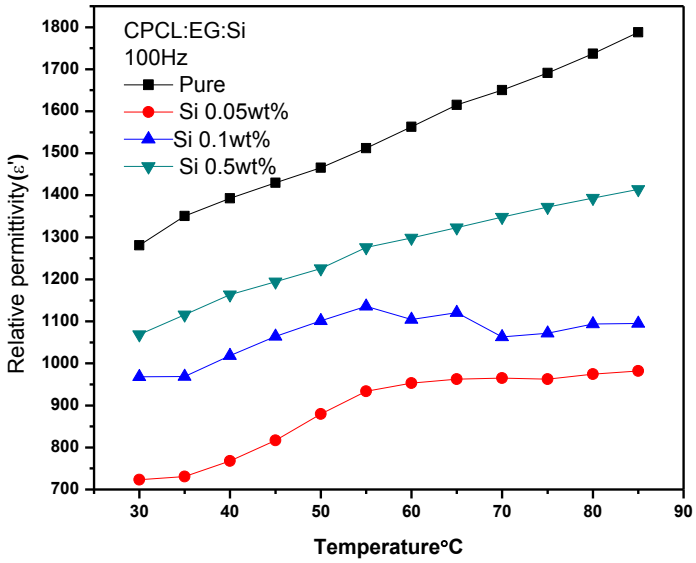

Figure 4.3(c): Variation of relative permittivity with temperature for CPCL:EG:Si systems at 100 Hz.

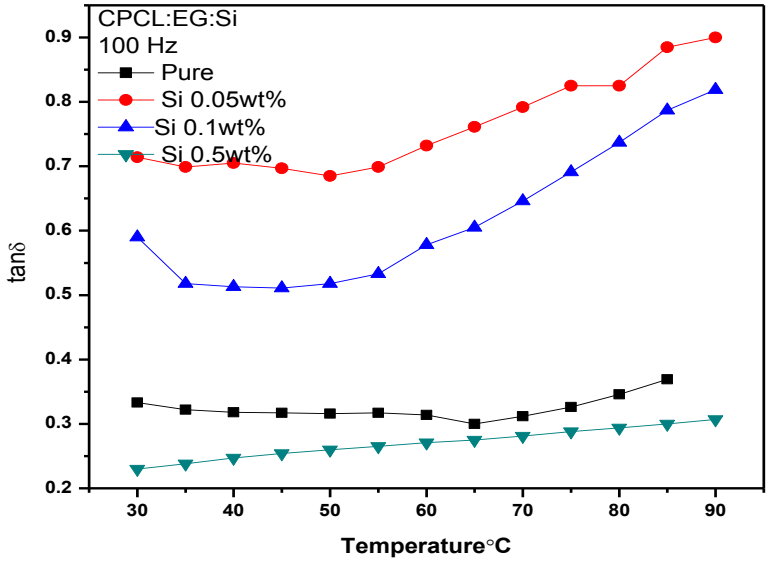

Figure 4.3(d): Variation of tanδ with frequency for CPCL:EG:Si systems at100 Hz.

Figure 4.3(c) shows the variation of relative permittivity as a function of temperature at 100 HZ. It was found that permittivity was higher in pure system and decreased with the

dispersion of nano particles. We observed that dielectric permittivity was increased with the temperature in pure system. Though, in dispersed system it gets saturated at higher temperature.

Figure 4.3(d) shows that tanδ v/s frequency plot. Loss is higher for the dispersed systems as compared to the pure. No significant variation with increasing temperature was seen.

4.3.2 Dielectric study of CTAB:EG:Si systems

The variation in relative permittivity (**ε'**) as function of frequency for pure (CTAB:EG) and silica nano particle dispersed samples are shown in figure4.3(e). We observed that CTAB:EG:Si system also displayed same behavior as observed in the CPCL:EG:Si system. The dispersion of the Si nano particles suppresses the relative permittivity of the system.

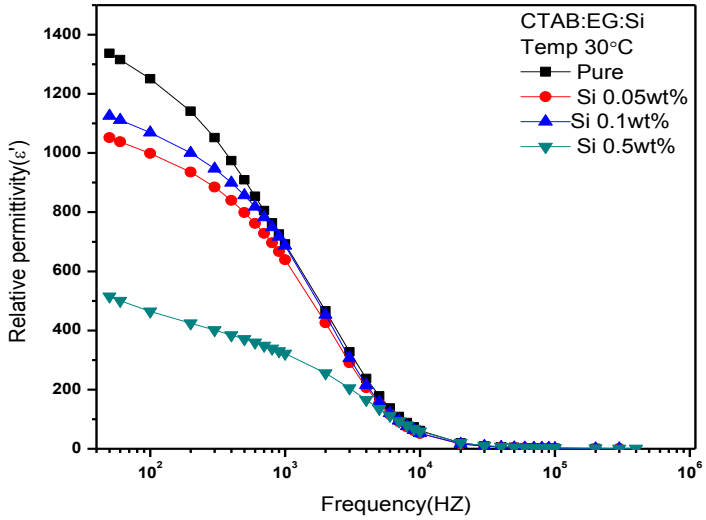

Figure 4.3(e) Variation of relative permittivity with frequency for CTAB:EG:Si systems room temp.

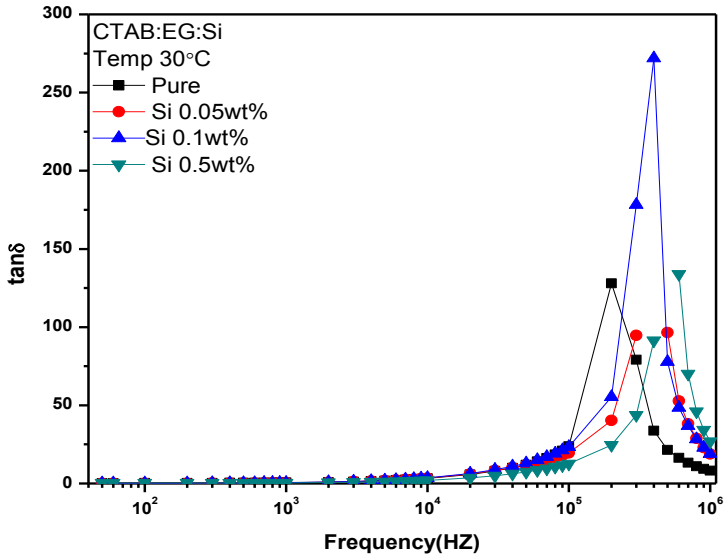

Figure 4.3(f) Variation of tanδ with frequency for CTAB:EG:Si systems room temp.

Fig. 4.3(f) shows that the plot, value of loss is low at lower frequency and increased as the frequency reached to higher value.

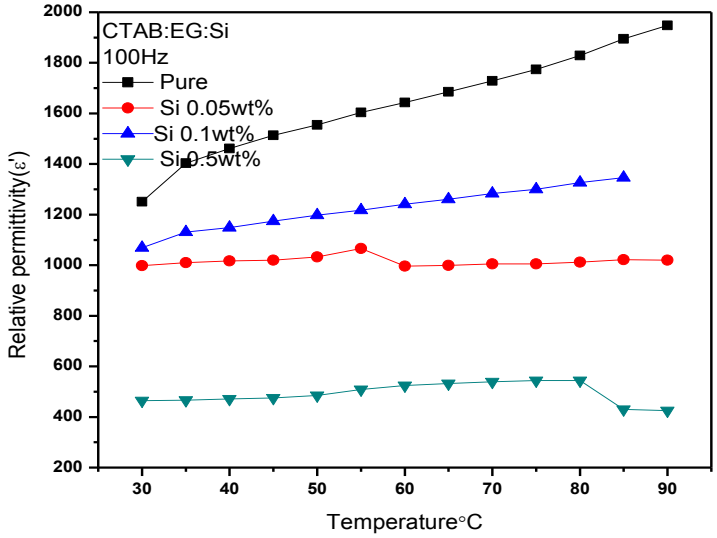

Figure 4.3(g): Variation of relative permittivity with temperature for CTAB:EG:Si systems at 100 Hz.

Figure 4.3(g) shows the variation in relative permittivity as a function of temperature at 100 Hz. At low frequency (100Hz) we found that the dielectric constant of pure system shows higher relative permittivity than that of dispersed mesophases. The permittivity was found to be increased in pure system with the variation of the temperature thought it shows almost constant behavior in the dispersed systems.

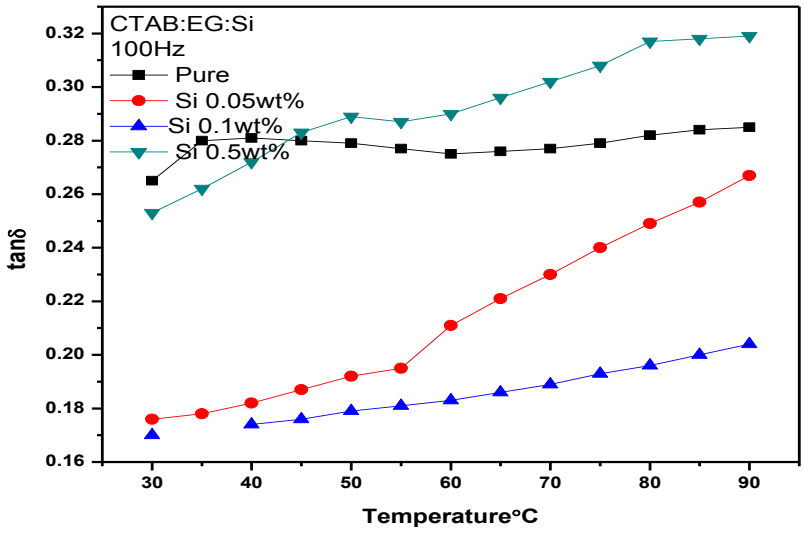

Figure 4.3(h): Variation of tanδ with frequency for CTAB:EG:Si systems at100 Hz.

In this frequency region loss is minimum for the dispersed system. Gradual increase in the loss was observed with the variation of the temperature.

4.3.3 Dielectric study of SDS:EG:Si systems

Frequency dependent of relative permittivity of SDS:EG:Si system are shown in figure 4.3(i) it is evident from the graph that pure SDS:EG system have low dielectric permittivity at lower frequency region, which further found to be increased with the addition of the Si nano particles upto si=0.1wt% and decreased at higher concentration. Such increase in the permittivity attributed to the strong coupling between Si particle and LLC molecules.

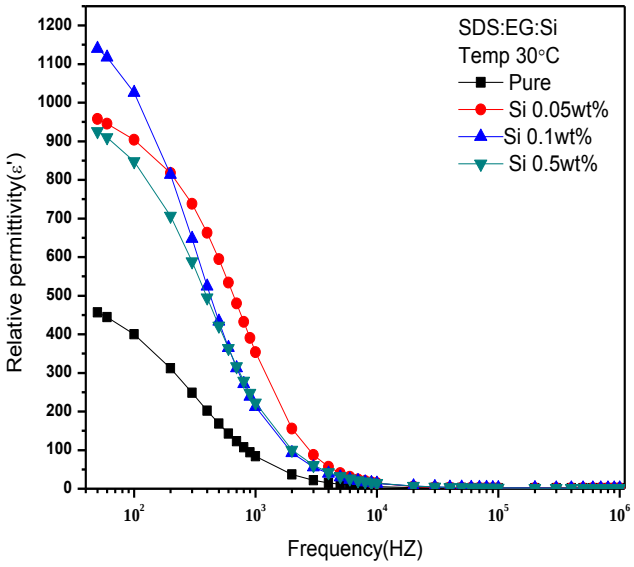

Figure 4.3(i): Variation of relative permittivity with frequency for SDS:EG:Si systems room temp.

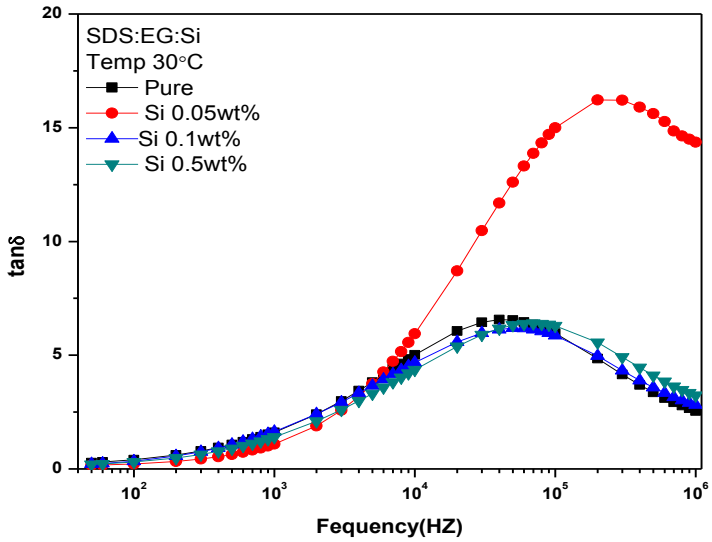

Figure 4.3(j) Variation of tanδ with frequency for SDS:EG:Si systems room temp.

Figure 4.3(j) shows the variation loss with frequency. it was observed that loss are minimum in lower frequency region which further increased in intermediate frequency zone and suppressed again at higher frequencies.

Figure 4.3(k) shows the variation of dielectric permittivity v/s temperature. we observed that dielectric constant increased upto 40℃ and then becomes almost constant in all the samples though, the magnitude is high in dispersed samples.

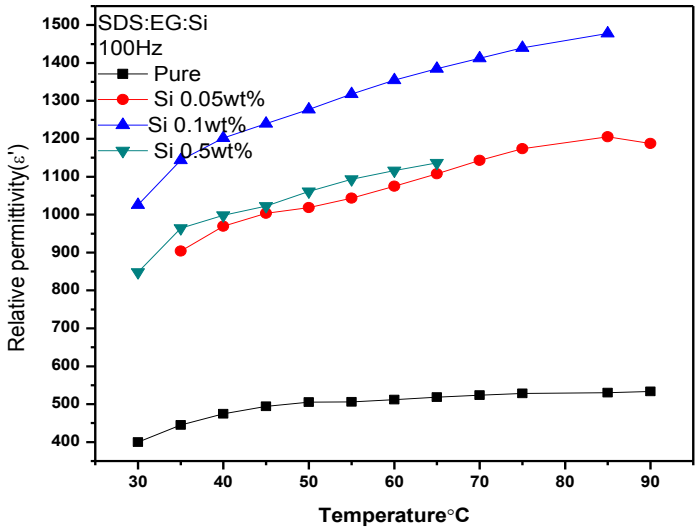

Figure 4.3(k): Variation of relative permittivity with temperature for SDS:EG:Si systems at 100 Hz.

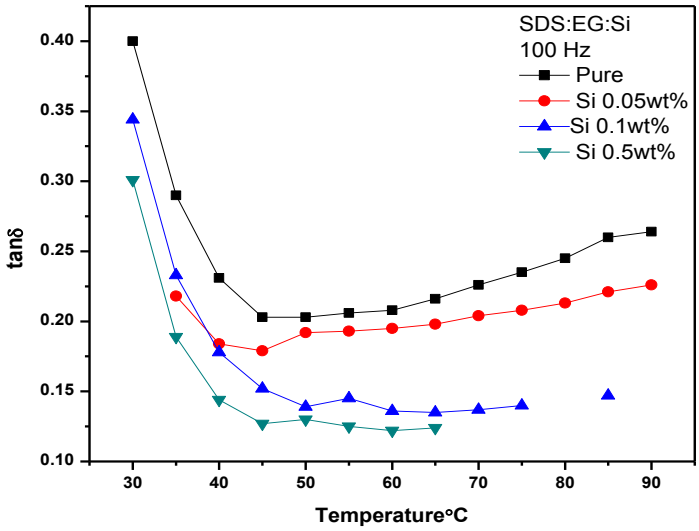

Figure 4.3(i): Variation of tanδ with frequency for SDS:EG:Si systems at100 Hz.

As shown in figure 4.3(i) the dissipation factor in SDS:EG system was much higher at low temperature range. It was found that loss become minimum near 40^0C and become constant up to higher temperature range.

4.3.4:Comparative dielectric study of all systems

4.3.4.1:All pure systems at room temperature

Figure 4.3(m) represent the variation of dielectric permittivity v/s frequency plot of all the pure samples. It was found that cationic system shows higher permittivity than that of anionic one.

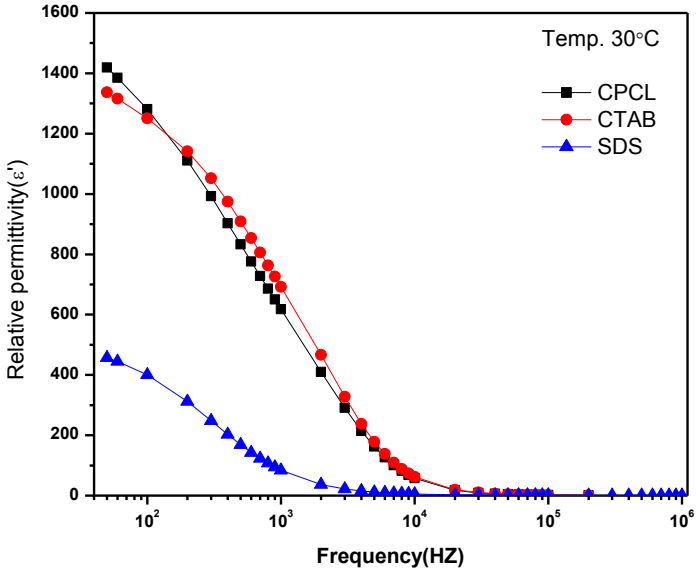

Figure 4.3(m): Variation of relative permittivity of all pure samples with respect to frequency at room temperature

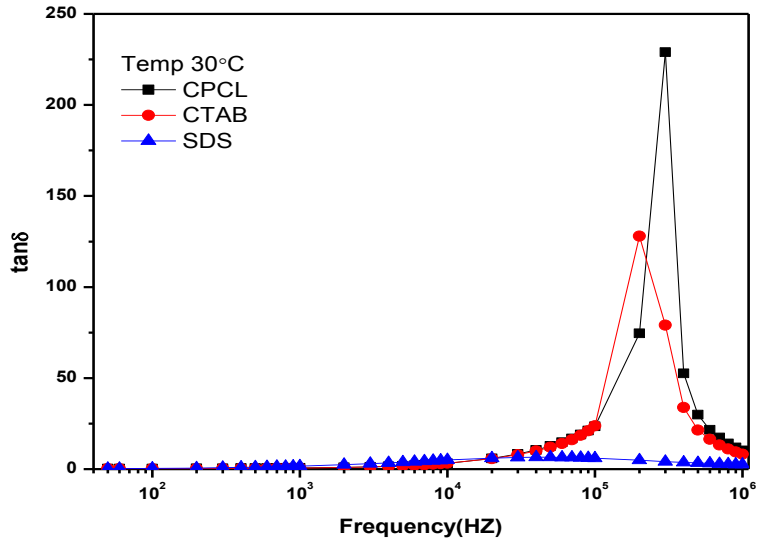

Figure 4.3(n): Variation of tanδ Vs frequency for all pure samples at room temperature.

The plot frequency v/s dissipation factor shows in figure 4.3(n) value of dissipation factor is low at lower frequency its value is increased at higher frequency.

4.3.4.2: All system of dispersed with Si 0.05%wt% at room temperature

The comparative beheaviour of the permittivity for all the systems at dispersed with 0.05wt% is shown in figure 4.3 (o). At very low concentration we found that the CTAB system shows higher permittivity than others.

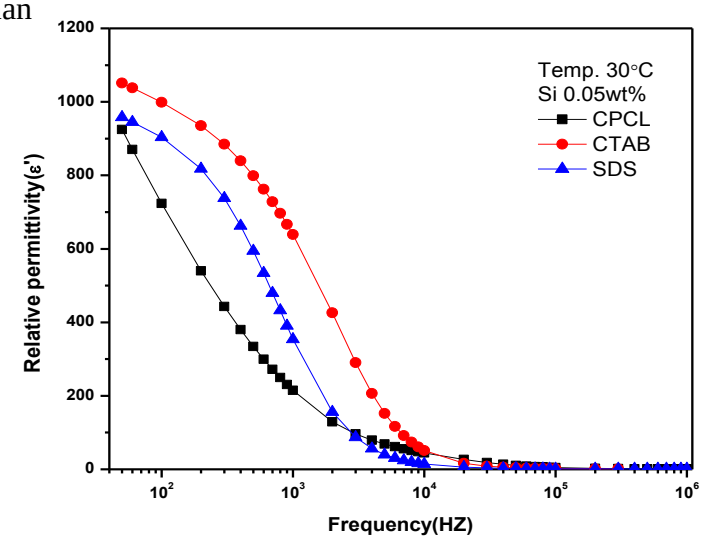

Figure 4.3(o): Variation of relative permittivity of all systems at Si 0.05% with respect to frequency at room temperature.

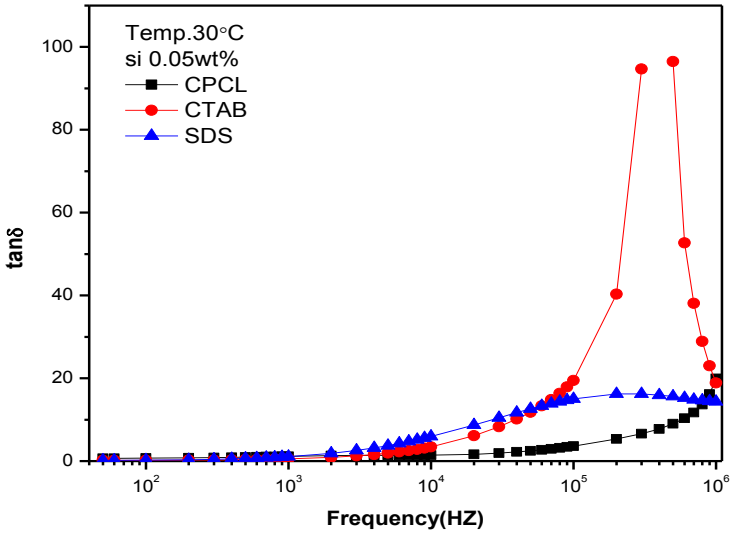

Figure 4.3(p): Variation of tanδ Vs frequency at room temperature for all systems dispersed with Si 0.05wt%.

Figure 4.3(p) shows the variation of loss different system (CPCL,CTAB and SDS) at Si 0.05wt% concentration the value of dissipation factor is lower at low frequency and its increase at higher frequency range. The loss is found maximum in CTAB based samples at this particular concentration.

4.3.4.3: All system of dispersed with Si 0.1%wt% at room temperature

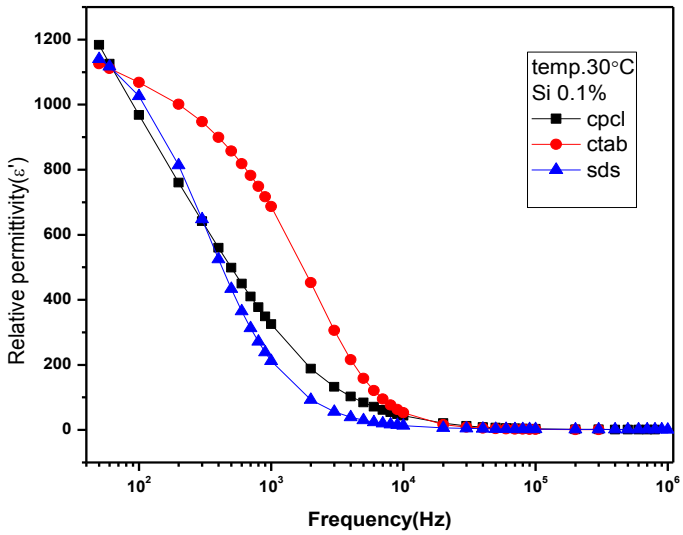

Figure 4.3(q): Variation of relative permittivity of all systems at Si 0.1% with respect to frequency at room temperature.

Figure 4.3(q) shows that the comparative beheaviour of all three LLC systems at Si 0.1wt% concentration. The values of CPCL system have high relative permittivity at low frequency range.

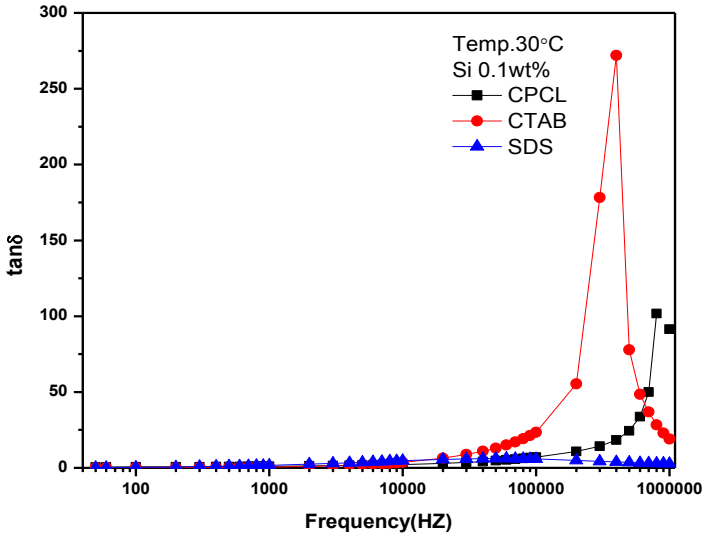

Figure 4.3 (r): Variation of tanδ Vs frequency at room temperature for all systems dispersed with Si 0.1wt%.

It was found that loss factor is lower at low frequency range and its increase at higher frequency range as evident from the figure.

4.3.3.4: All systems of Si 0.5wt% at room temperature

In comparison to lower concentrations at higher concentration CPCL have higher magnitude of relative permittivity than others as shown in figure 4.3(p).

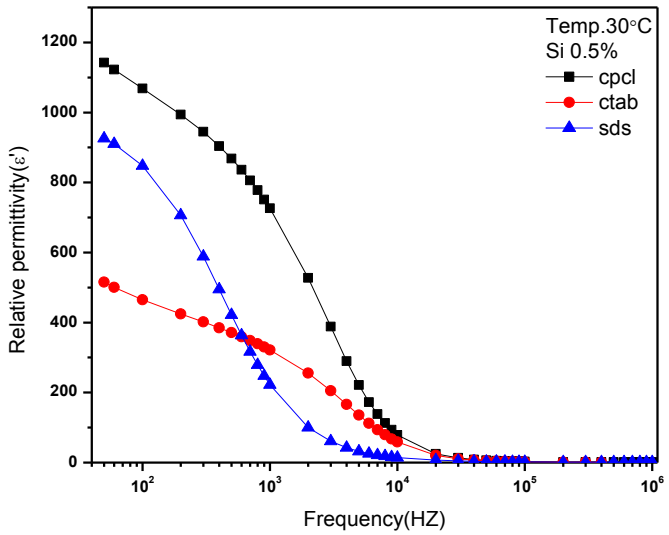

Figure 4.3(s): Variation of relative permittivity of all samples at Si 0.5% with respect to frequency at room temperature.

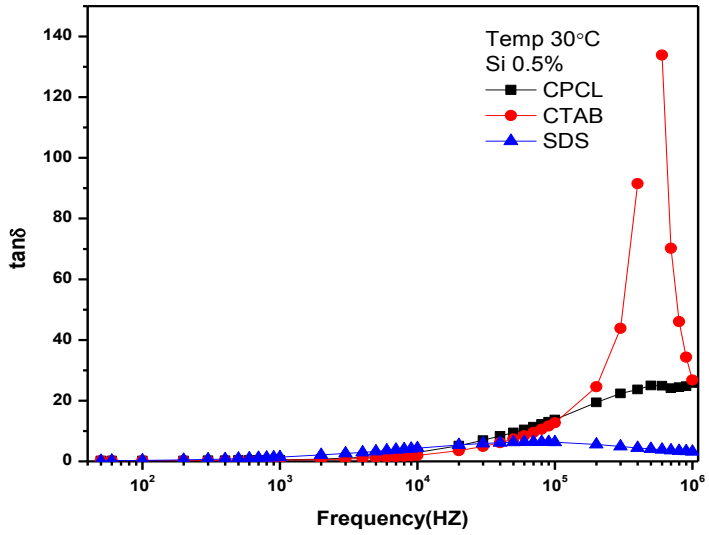

Figure 4.3 (t): Variation of tanδ Vs frequency at room temperature for all systems dispersed with Si 0.5wt%.

The value of loss factor in different LLC system is lower at low range of frequency. And it increase at higher frequency range. The value of loss factor is maximum in CTAB:EG system at high frequency range.

4.4. Chemical analysis by FTIR spectroscopy

The synthesized binary and ternary mixtures were characterized by FTIR to understand any kind of chemical change in these systems.

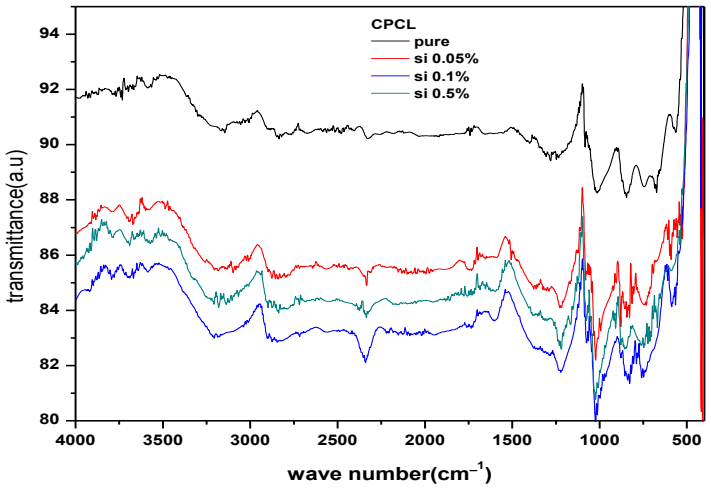

Figure 4.4(a): FTIR spectra of CPCL:EG pure and Si particle dispersed systems

Figure 4.4(a) display the IR spectra of the CPCL:EG:Si systems. We observed the major reflection at around 3200,2850 and 2400 cm^{-1} corresponding to the O-H, C-H and C-C bonds of the CPCL:EG. No new bond formations have been found in any case revealing that there is no chemical reaction taking place in these chemical species.

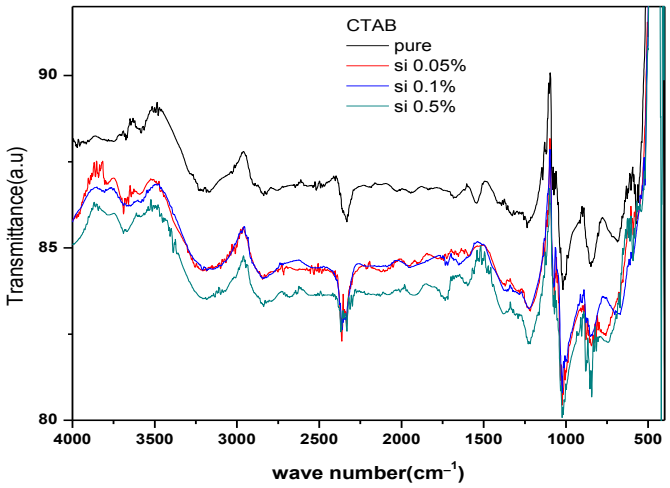

Figure 4.4(b): FTIR spectra of CTAB:EG pure and Si particle dispersed systems

Figure 4.4(b) present the FTIR spectra of the CTAB:EG:Si system. Band observed at 3700, 3200, 2800 and 2400 corresponding to the N-H, O-H, C-H and C-C respectively.

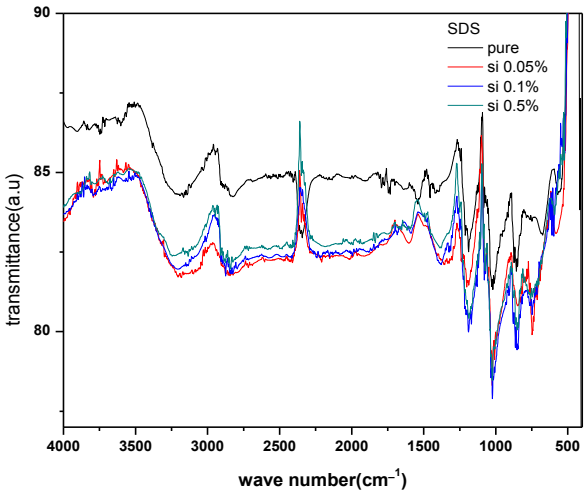

Figure 4.4(c): FTIR spectra of SDS:EG pure and si particle dispersed systems

Figure 4.4(c) shows the IR spectra of the SDS:EG:Si system. Peaks observed at 3300, 2550 and 2400 cm^{-1} which corresponds to the O-H, C-H and C-C bond.

From IR analysis it can be concluded No new bond formations have been found in any case revealing that there is no chemical reaction taking place in these chemical species. Efforts are on for more analysis of these complex IR spectra to conclude more about these systems. Modification in the physical properties is due to the interfacial interaction of Si nano particle and LLC mesophases.

Conclusions

1.All the systems (cationic and anionic) shows well defined four lobe texture in pure and Si dispersed samples at lower and higher concentration of the dopant confirming that addition of nano particles does not disturbing the ordering of the LLC systems.

2. XRD analysis inferring that addition of Si nano particles does not affect the structure of the parent LLC phases obtained from cationic and anionic surfactants at any concentration. Interestingly lamellar to hexagonal transition has been noticed in CTAB:EG system at higher concentration of Si(0.5wt%). Such transition in the LLC phase may be due to the increase in the optimal surface area of the head group, which produce undulation in the layers of lamellas and boost the micelles get packed in hexagonal array.

3. Dielectric studies reveals that addition of Si particles suppress the permittivity of LLC phases derived from cationic surfactant (CPCL and CTAB), however, reverse effect has been noticed in the LLC phases obtained from the anionic surfactant (SDS).

4. No significant information has been found from the chemical analysis. It requires more analysis to reach at finally conclusion to confirm the any kind of chemical interactions in these complexes.

REFERENCES

1. P. G. de Gennes and J. prost, The Physics of liquid crystals, Clarendon Press, Oxford, (1993).
2. T. P. Hoar and J. H. Schulman, Nature (London) 152, 102, (1943).
3. L. M. Prince (Ed.) Microemulsions, Theory and practice, Academic Press, New York, (1976).
4. I. Danielsson and B. Lindman, Colloid. Surf. 3, 391, (1981).
5. C. J. F. Bottcher and P. Bordewijk, Theory of electric polarization, Elsevier, Amsterdam, (1978).
6. C. Tanford, The Hydrophobic effect: Formation of micelles and biological membranes, Wiley, New York (1980).
7. D. Mirkovitsi, A. Mathis, J. Simon, J. C. Wittman, and J. Le Moigne, Mol. Cryst. 64, 121, (1980).
8. J. N. Isreaelachvili, D. J. Mitchell, and B. w. Ninham, J. Chem. Soc.Faraday Trans. 272, 1525, (1976).
9. W. C. Preston, J. Phys. Collioid Chem. 52, 84, (1968).
10. R. G. Laughlin, the aquous phase behaviour of surfactant, Academic Press, London,(1994).
11. L. B. Johansson, O. oderman, J. Phys. Chem., 91, 5275, (1987).
12. J. Israelachvili, H. Wannerstrom, Langmuir, 6, 873, (1990).
13. J. H. Clint, surfactant aggresation, Blackie, Glasgow, (1990).
14. H. Hagslatt, O. Soderman, B. Jonsson, 10, 2177, (1994).
15. Z. X. Li, E. M. Lee, R. K. Thomos, J. Penford, J. Colloid Int. Sci. 187, 492, (1997).
16. C. Tanford, The hydrophobic effect: Formation of micelles and biological membranes, Wiley Interscience, New York, (1980).
17. B. Kronberg, M. Costas, R. Silverston, J. Disp., SciTechnol,. 15 (3), 333, (1994).
18. Muscutariu, Cristale lichide si aplicatii, Ed. Tehnica, bucarest, (1981).
19. R. L.ipowsky, E. Sakman, Eds., Handbook of biological physics, vol. 1b, Structure and dynamics of membrane, Generic and specific interactions, Elsevier Science, Netherlands, (1995).

20. P. Sakya, J. M. Seddon, R. H. Templer, R. J. Mirkin, G. J. T. Tiddy, Langmuir, (1997).
21. A. Gulik, H. Delacroix, Kischner, V. Luzatti, J. Phys. 2 France, 5, 445, (1995).
22. V. Luzatti, P. A. Spegt, Nature, 215, 707, (1976).
23. A. Tardieu, V. Luzatti, Biochim. Bio. Phys. Acta, 11, 219, (1970).
24. K. D. Lawson, T. J. Flautt, Magnetically oriented lyotropic liquid crystal phases. J. Am. Chem. Soc. 89, 5489, (1967).
25. N. Boden, R. Y. Bushby, C. Hardy, J. de Phys. Lett. 46, 325, (1985).
26. M. Menti, G. Barbero, G. Bartolino, T. Chiaranza, E. Semoni, Nuovo Cimento. Ser. D. 3, 30 (1984).
27. M. C. Holmes, P. Sotta, Y. Hendrix, B. Deloche, J. de Phys. 2 France, 1735, (1993).
28. J. Galerne, J. P. Marcerou, Temperature concentration behaviour of the order of the order parameter in the nematic phase of a lyotropic liquid crystal, Phys. Rev. E 23, 2109, (1983).
29. I. Furo, B. Halle, J. Chem. Phys. 91, 42, (1989).
30. S. Emid, J. Konijnendijk, J. Smidt, A. Pines,, Physica, B 100, 215, (1980).
31. I. Furo, B. Halle, L. Enarsson, Chem. Phys. Lett. 182, 547, (1991).
32. N. Boden, K. Radely, M. C. Holmes, Mol. Phys., 42, 493, (1981).
33. Y. Hendrix J. Charvolin, M. Rawiso, L. Liebert, M. C. Holmes, Anisotropic aggregates of amphiphilic molecules in lyotropic nematic phase, J. Phys. Chem., (1983).
34. R. K. Shukla, K. K. Raina Int. J. Mod. Phys. B. 23, 5075, (2009).
35. Caiqi Wang, Yuping Dong, Huimin Tan, Carbohydrate Research 338, 535–540, (2003).
36. Wilson Quevedo, chrustuan Peth, Gerhard Busse, Int. J. Mol. Sci, 10, 4754, (2009).
37. P. Pieranski, L. Sittler, P. Sotta and Imperor Clerc Eur. Phys. J. E 5, 317 (2001).
38. Ali Khana, F. Eduardo, B. Marquesa, current opinionium colloid & Interface Sci. 4, 402, (2000).
39. Hironobu Kunieda, Kazuki Shigeta, and Kazuyo Ozawa J. Phys. Chem. B 101, 7952 (1997).
40. X. auvray, T. Perche, C. Petipas, and R. Anthore, Langmuir, 8, 2611, (1992).